

Common-mode voltage mitigation in multiphase electric motor drive systems

Endika Robles^{a,*}, Markel Fernandez^a, Jon Andreu^a, Edorta Ibarra^a, Jordi Zaragoza^b, Unai Ugalde^a

^a University of the Basque Country (UPV/EHU), Faculty of Engineering, Plaza Ingeniero Torres Quevedo 1, 48013 Bilbao, Spain

^b Terrassa Industrial Electronics Group, Technical University of Catalonia, 08222 Barcelona, Spain

ARTICLE INFO

Keywords:

Electric drives
Common-mode voltage
Power conversion topologies
Inverter
Multiphase
Modulation
PWM

ABSTRACT

Common-mode voltage (CMV) produces serious reliability and electromagnetic interference (EMI) issues in modern pulse-width modulated (PWM) electric drives. Such issues will become more prominent in the near future, as industry moves towards the introduction of wide-bandgap (WBG) semiconductor technologies operating at higher switching frequencies and also with greater dv/dt . In this context, multiphase electric drive technologies can be of great interest, as their additional degrees of freedom can be exploited to reduce CMV. This work aims to study the potential of multiphase electric motor drive systems for CMV mitigation. To do so, a comprehensive review of the most recent scientific literature is conducted, mainly focusing on high impact works published recently. As a result, a clear and up-to-date picture of the most common multiphase technologies, i.e., $(m+1)$ -leg, multiple three-phase, open-end and star-connected multiphase systems is provided along with their CMV reduction potential. Not only the topologies themselves but also modulation techniques are analysed and presented, mainly focusing on star-connected systems. As a conclusion, it can be stated that such multiphase systems are promising candidates to substitute conventional three-phase motor drives as, apart from their well-known advantages (efficiency, power density, power splitting, and fault tolerance), their CMV reduction potential is confirmed. The technical information provided in this work will help researchers and field engineers to design and develop high-performance multiphase electric drives.

1. Introduction

In industrial processes, it is usual for mechanical energy demands to be mostly satisfied by electric motor driven systems (EMDSs). Among these, fans [1,2], pumps [3,4] and compressors [5,6] accounted for almost 85 % of this overall demand over these last years [7]. In the transport sector, however, it was not until recently that fuel-powered engines have started being replaced by electric powertrains. A paradigm shift is under way here: passenger electric vehicle (EV) sales jumped from 450,000 in 2015 to 2.1 million in 2019, and this market is forecasted to grow up to 26 million sales by 2030 and even to 54 million sales by 2040 [8]; see Fig. 1.

This increasingly widespread use of EMDSs resulted in electric motors consuming about 40 % of the worldwide energy supply in the former decade [9–11], and up to 70 %–90 % in the industrial sector [6,12]. This has brought the corresponding environmental problems and global warming issues to the fore: national governments are gradually adhering to Minimum Energy Performance Standard specifications [13], and international standardization organizations are

constantly reviewing relevant documents, e.g. IEC61800-9 — “Ecode-sign for power drive systems, motor starters, power electronics and their driven applications” [12,14,15]. This picture is confirmed by various market studies and scientific papers, which point out that the topmost concerns of electric drive users are energy efficiency and maintenance costs, closely followed by reliability, safety and robustness [9, 10,16–18].

Modern electric drives (Fig. 2) provide an excellent performance in terms of system efficiency, controllability, quality of the synthesized waveforms and robustness. This is achieved by incorporating a power converter that includes several semiconductor devices to feed the electric machine. Power converter alternatives are generally classified into two categories: current source inverters (CSI) and voltage source inverters (VSI). CSIs have a number of advantages such as a simple current control scheme, short circuit protection and the absence of capacitors to constitute the DC-link [19]. However, the disadvantages of CSIs are relevant for electric drive applications: (i) a front-end converter (or, at least, a bulky series inductance) is required to synthesize

* Corresponding author.

E-mail addresses: endika.robles@ehu.eus (E. Robles), markel.fernandez@ehu.eus (M. Fernandez), jon.andreu@ehu.eus (J. Andreu), edorta.ibarra@ehu.eus (E. Ibarra), jordi.zaragoza-bertomeu@upc.edu (J. Zaragoza), unai.ugalde@ehu.eus (U. Ugalde).

<https://doi.org/10.1016/j.rser.2021.111971>

Received 9 February 2021; Received in revised form 28 October 2021; Accepted 29 November 2021

Available online 31 December 2021

1364-0321/© 2021 The Author(s).

Published by Elsevier Ltd.

This is an open access article under the CC BY-NC-ND license

(<http://creativecommons.org/licenses/by-nc-nd/4.0/>).

Nomenclature

M_a	Amplitude modulation index
N_L	Number of different CMV steps per T_{sw}
N_T	Number of CMV transitions per T_{sw}
SW_x	Main switch with number of branch x
SW'_x	Complementary switch with number of branch x
THD_i	Total harmonic distortion of the output current (%)
T_{SW}	Switching period or modulation period (s)
v_{CM}	Common-mode voltage (V)
V_{DC}	DC bus voltage (V)
\mathbf{V}_{ref}	Reference voltage vector
\mathbf{V}_x	x vector
v_{x0}	x phase-to-ground voltage (V)
Δ_P	Peak-to-peak relative value of CMV waveform
Δ_S	Height of largest relative value of CMV step

Abbreviations/acronyms

AC	Alternating current
AZS-PWM	Active zero-state PWM
CB	Carrier-based
CCMV-PWM	Constant CMV PWM
CSI	Current-source inverter
CMV	Common-mode voltage
DC	Direct current
D-PWM	Discontinuous PWM
EMDS	Electric motor driven systems
EMF	Electro-motive force
EMI	Electromagnetic interferences
EV	Electric vehicle
HVDC	High-voltage DC
IMPC	Improved MPCC
MPC	Model predictive control
MPCC	Model predictive current control
NS-PWM	Near-state PWM
PWM	Pulse-width modulation
RCMV-PWM	Reduced CMV PWM
RS-PWM	Remote-state PWM
SV	Space-vector
SV-PWM	Space-vector PWM
VSI	Voltage-source inverter

a constant DC-link current [20]; (ii) output filters must be included as high output current harmonics are produced [21]; and (iii) high torque ripple is generated due to the chopped current if an adequate filter is not used [14]. For all these reasons, in general it is uncommon to find CSIs in electric drive systems [20].

In contrast, VSIs exhibit many advantages for electric drive applications. While in CSIs the DC-link current is modulated at the output side of the converter, in VSIs the output voltage is modulated. This allows the direct connection of the VSI to the input (voltage source) and output (inductive load) without requiring input inductors or output filters.¹ For

¹ VSIs usually incorporate an input capacitor or capacitor bank which, in any case, is cheaper and less bulky than the input side inductance required for a CSI.

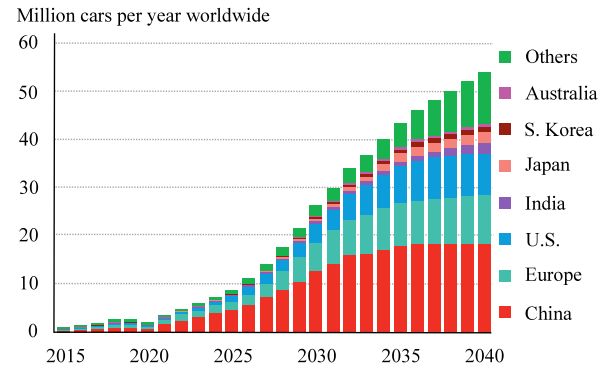


Fig. 1. Annual passenger EV sales by region [8].

this particular reason, VSI architectures greatly reduce the volume and weight of the drive, a factor that is critical for certain applications such as for electric vehicles.² Furthermore, the advances carried out during the last decades in power semiconductor technologies (typically silicon IGBTs that switch at high frequencies) have consolidated VSIs as the most common alternative for electric drives [4,20,22,23].

Depending on the arrangement of the power semiconductors and reactive elements, several VSI topologies of n -levels and m -phases can be constituted, which are commonly classified as:

1. *Two-level three-phase inverters* (Fig. 2). These are the most common ones, and have been widely investigated in the scientific literature. For example, control and modulation strategies for these converters have reached a considerable maturity [24–29]. In [30], authors have carried out a comprehensive literature review on CMV issues and mitigation strategies for two-level three-phase VSIs.
2. *Multilevel inverters*. These topologies ($n \geq 3$) provide more than two output voltage levels per phase, allowing the VSI to operate with voltages higher than the ones imposed by the semiconductor device technology [46]. In addition, multilevel converters provide other benefits such as an improved output waveform quality (total harmonic distortion of the output current $-THD_i$, lower than in two-level inverters), lower electromagnetic interferences (EMI) and fault tolerance [11,47]. For these reasons, a relevant number of multilevel solutions have been investigated and industrialized in last decades, where the most well-known multilevel converter topologies are the Neutral-point-clamped (NPC) [32,33], the Flying capacitor (FC) [34,37], the Cascaded H-bridge (CHB) [40,42] and the Modular multilevel (MM) converter [43,44]. Table 1 summarizes their most relevant features along with a number of references that deal with multilevel inverters and CMV.
3. *Multiphase inverters*. These topologies ($m > 3$) bring many performance benefits [48–50], such as power splitting between phases (lower currents for the same rated power), improved efficiency, higher power density, lower output current ripple, lower electromagnetic interference (EMI), additional control degrees of freedom, an intrinsic fault tolerance and therefore improved reliability [51–54]. Consequently, although system complexity is increased, multiphase VSIs are becoming attractive in a wide range of applications, particularly when high power density or uninterrupted operation is required, e.g. in-wheel electric vehicle drives [55], ship propulsion [56], and life-critical aerospace systems [57].

² In electromobility applications, where there is a voltage source at the input side of the converter and the load is inductive, it makes no sense to use a CSI topology, as this last would require incorporating additional reactive elements, significantly reducing system performance.

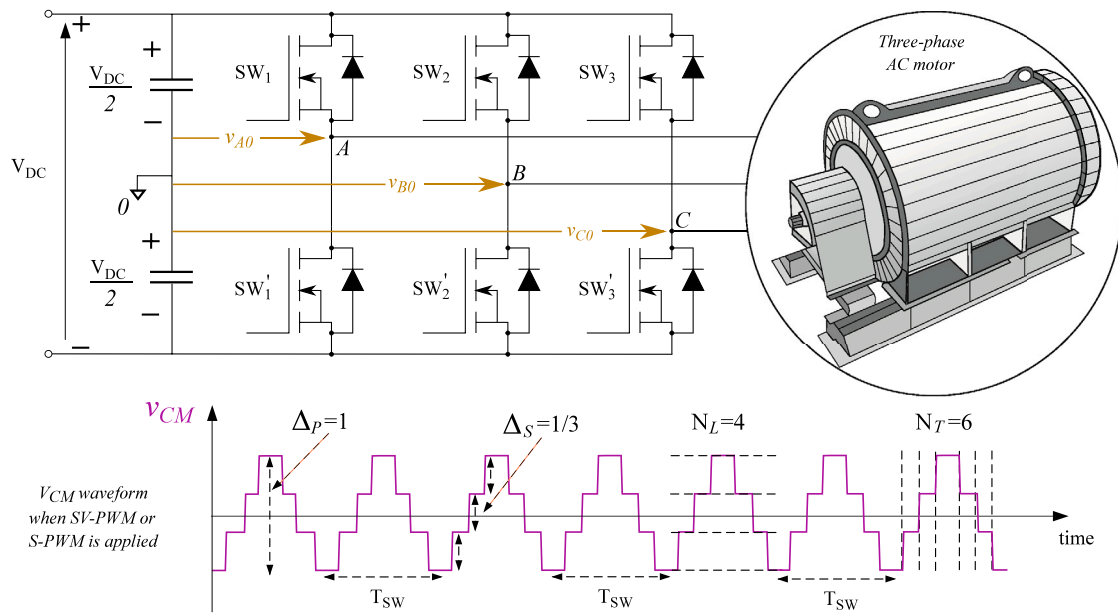


Fig. 2. Top: Two-level three-phase VSI motor drive system. Bottom: CMV waveform synthesized by SV-PWM.

Table 1

Features of the most relevant multilevel inverter topologies and summary of references that investigate the CMV phenomenon and mitigation techniques in such architectures.

	Neutral-point-clamped	Flying capacitor	Cascaded H-bridge	Modular multilevel
Advantages	<ul style="list-style-type: none"> • Single DC-link voltage source. • Fewer capacitors than FC. • Economical for low levels. 	<ul style="list-style-type: none"> • Single DC-link voltage source. • Redundant switching states: fault tolerance. • Low number of active devices. 	<ul style="list-style-type: none"> • Modular structure. • Easier to provide high voltage. • Redundant switching states. • High fault tolerance. 	<ul style="list-style-type: none"> • Great modularity. • Redundancy and reliability. • Absence of extra DC-link capacitors. • High efficiency.
Disadvantages	<ul style="list-style-type: none"> • Active balance required for DC-link capacitors. • Unbalanced switching losses. • High blocking voltage in the clamping diodes. • Low frequency ripple in the neutral point (for $\uparrow M_a$ and \downarrow power factor). 	<ul style="list-style-type: none"> • Very bulky when the number of levels is increased. • Pre-charge is required in the capacitors. • Reduced modularity. • Expensive. 	<ul style="list-style-type: none"> • High number of isolated DC sources. • Voltage imbalance between phases. 	<ul style="list-style-type: none"> • Higher capacitor voltage ripple. • Complex system with multiple variables to control.
CMV references	[31–33]	[34–37]	[38–42]	[43–45]

All these VSI converters (regardless of the number of levels (n) and phases (m)) are controlled with the corresponding PWM technique (either carrier-based (CB-PWM) [27,29] or vector space (SV-PWM) [26,28]) to generate a sinusoidal output current in the motor.³ PWM-based sinewave generation is well known to produce a common-mode voltage (CMV) component [60–63]. The resulting CMV waveforms (Fig. 2) cause several issues, such as high EMI [64–66], deterioration of the electric machine stator winding insulation [67,68], and pitting and fluting of its bearings [24,69–71]. Furthermore, this latter damage will likely be aggravated as a result of the introduction of power devices made of wide-bandgap semiconductors, instead of silicon-based devices, due to their ability to handle higher switching frequencies, which would therefore accelerate the ageing of the bearings [24,72]. Indeed, Fig. 3 illustrates the breakthrough that is currently under way in the

³ Two-level three-phase CSI converters produce lower levels of CMV than two-level three-phase VSI converters because the coil connected to the DC-link filters this voltage. In addition, since these converters are controlled by current, the modulation scheme does not generate a pulsing voltage signal in each phase of the converter, but rather sinusoidal [58,59].

semiconductor industry, as silicon carbide and gallium nitride-based devices have already gained a substantial market share [73].⁴

Multilevel converters can be considered as great candidates for CMV reduction as, unlike traditional VSIs and other converter topologies, they can produce 0 V CMV levels using a suitable modulation technique [32,35,39]. However, this is achieved at the cost of worsening other figures such as the output current harmonic distortion, efficiency or linear range. In this sense, multiphase converters are presented as an alternative to multilevel converters, as they have additional degrees of freedom that can also be used to reduce CMV. The singularities of multiphase inverters, and their particular suitability for certain important applications, call for a specific review of the relevant literature. Thus, the aim of this paper is to provide a complete survey of the existing alternatives to mitigate and ultimately suppress the presence of CMV variations in multiphase drives.

⁴ The incorporation of wide-bandgap devices on the market is a reality; however, today they are not mature enough to replace completely silicon. There is still a long way to go, solving problems at the device level, both in manufacturing, cost, and in performance (e.g. oscillations during device turn on). It can be said that the theoretical performance that such devices has not been yet achieved.

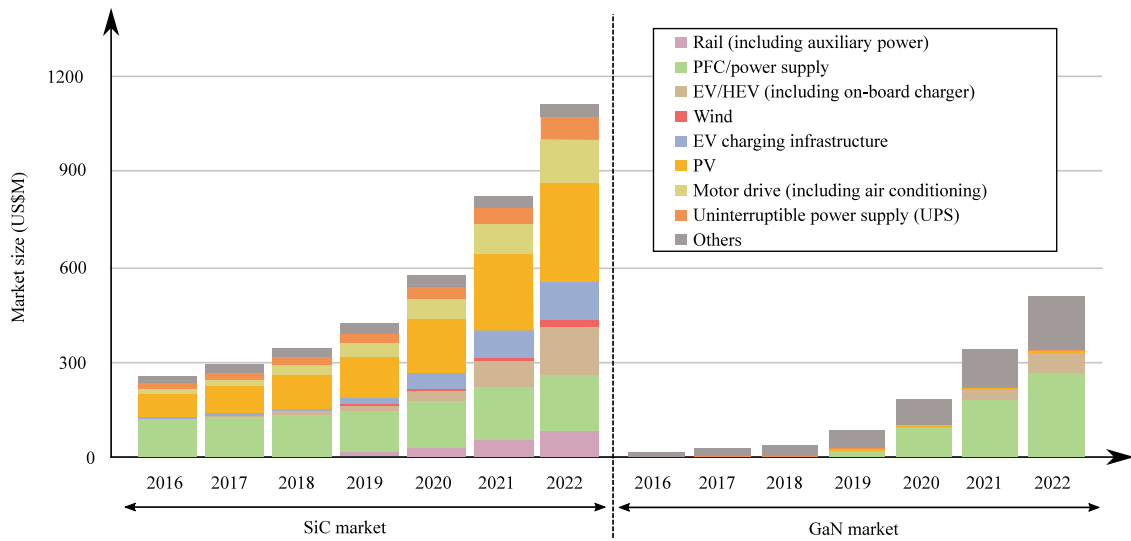


Fig. 3. Current SiC and GaN market status and future prospects, depending on the applications [73].

The paper is organized as follows: Section 2 summarizes how the CMV affects the conventional three-phase VSI, because the basic concepts can be extended to multiphase topologies. Next, Section 3 particularizes the main issues to multiphase topologies. The most relevant multiphase topology variants are reviewed, and a general picture of the CMV and its mitigation is provided for such systems. Then, star-connected multiphase solutions are identified as the ones exhibiting the best trade-off between CMV mitigation capabilities and complexity. Thus, Section 4 studies, in deep, the impact of various PWM modulation techniques specific to star-connected multiphase systems, pointing out their pros and cons as far as CMV is concerned. Finally, Section 5 draws the main conclusions of this review, highlighting the most significant features of each solution, in the belief that it will be a useful reference for academic researchers and practising engineers in the field of power electronics and energy conversion.

2. PWM-generated common-mode voltage in two-level three-phase inverters

All the CMV-related concepts in two-level three-phase voltage-source converters were formerly addressed by the authors in a previous work [30]. However, it is worth revisiting the most fundamental concepts prior deepening in the multiphase scenario.

When considering the conventional VSI converter of Fig. 2, which is virtually grounded at half the DC-link voltage ($V_{DC}/2$) and powering an AC motor, the CMV is defined as:

$$v_{CM}(t) = \frac{v_{A0} + v_{B0} + v_{C0}}{3}. \quad (1)$$

If the SV-PWM modulation technique is used, the CMV waveform of Fig. 2 [30] is obtained.⁵ Table 2 shows the voltage levels of this waveform, where each CMV level depends on the applied switching state. Among all these vectors, zero vectors are those that produce the highest levels of CMV, i.e. $\pm V_{DC}/2$. For this reason, most alternative topologies and modulation-based solutions are intended to avoid or minimize the application of zero vectors to reduce the CMV [25,26,28,74]. All the aforementioned software and/or hardware mitigation solutions provide particular CMV waveforms. Therefore, to better understand how the CMV affects an electric motor drive, it is of interest to compare different

⁵ This also occurs for carrier-based modulation techniques. The same waveform is also obtained with the carrier-based equivalent modulation technique that injects a third harmonic voltage following the min-max approach.

Table 2

CMV of traditional VSI converter according to the switching states and vectors associated with SV-PWM.

Voltage vector (switching state)	Device switching state			CMV [V]
	SW_1	SW_2	SW_3	
V_0 (000)	OFF	OFF	OFF	$-V_{DC}/2$
V_1 (100)	ON	OFF	OFF	$-V_{DC}/6$
V_2 (110)	ON	ON	OFF	$V_{DC}/6$
V_3 (010)	OFF	ON	OFF	$-V_{DC}/6$
V_4 (011)	OFF	ON	ON	$V_{DC}/6$
V_5 (010)	OFF	OFF	ON	$-V_{DC}/6$
V_6 (101)	ON	ON	OFF	$V_{DC}/6$
V_7 (111)	ON	ON	ON	$V_{DC}/2$

CMV patterns. As an example, the patterns shown in Fig. 4 (labelled as ①, ② and ③) are analysed. All these waveforms have been obtained by means of simulation considering the conditions depicted in Fig. 4(q).

Figs. 4(a)–4(c) show the CMV waveform, in time domain, obtained over a switching period (T_{SW}). Figs. 4(d)–4(f) show the CMV harmonics ranging from 0 to 80 kHz for a complete synthesized output voltage period (20 ms). Figs. 4(g)–4(i) show the harmonics, but over a wider frequency range, on a logarithmic scale, and in dB μ V. At first glance, this last representation may not seem very useful for comparison purposes. However, when talking about conducted EMI, this representation is the most common [61,64,66,72].

As previously mentioned, due to variations in CMV and to the existence of stray capacitances, unwanted leakage currents are produced which, among other things, damage motor bearings [30]. Therefore, if only the CMV waveform in time domain is considered, pattern ② is the best of the three analysed ones (Figs. 4(a)–4(c)) (less number of dv/dt). However, the opposite occurs when the frequency responses are considered to analyse the harmonic energy. To quantify the normalized energy of this voltage and, thus, to be able to determine which of the waveforms of the CMV is better, (2) is proposed in [68], where $x(i)$ is i th harmonic of the CMV.

$$E_{norm}(CMV) \approx \sum_{i=1}^{\infty} \left[\frac{x(i)}{V_{DC}/2} \right]^2. \quad (2)$$

According to this expression, pattern ③ seems to be a better alternative than ② (Table 3). However, this is only true when analysing the spectral voltage components, especially in terms of EMI. In this particular case, it is important to distribute the energy spectral density uniformly, that is, to limit the amplitude of the fundamental harmonics.

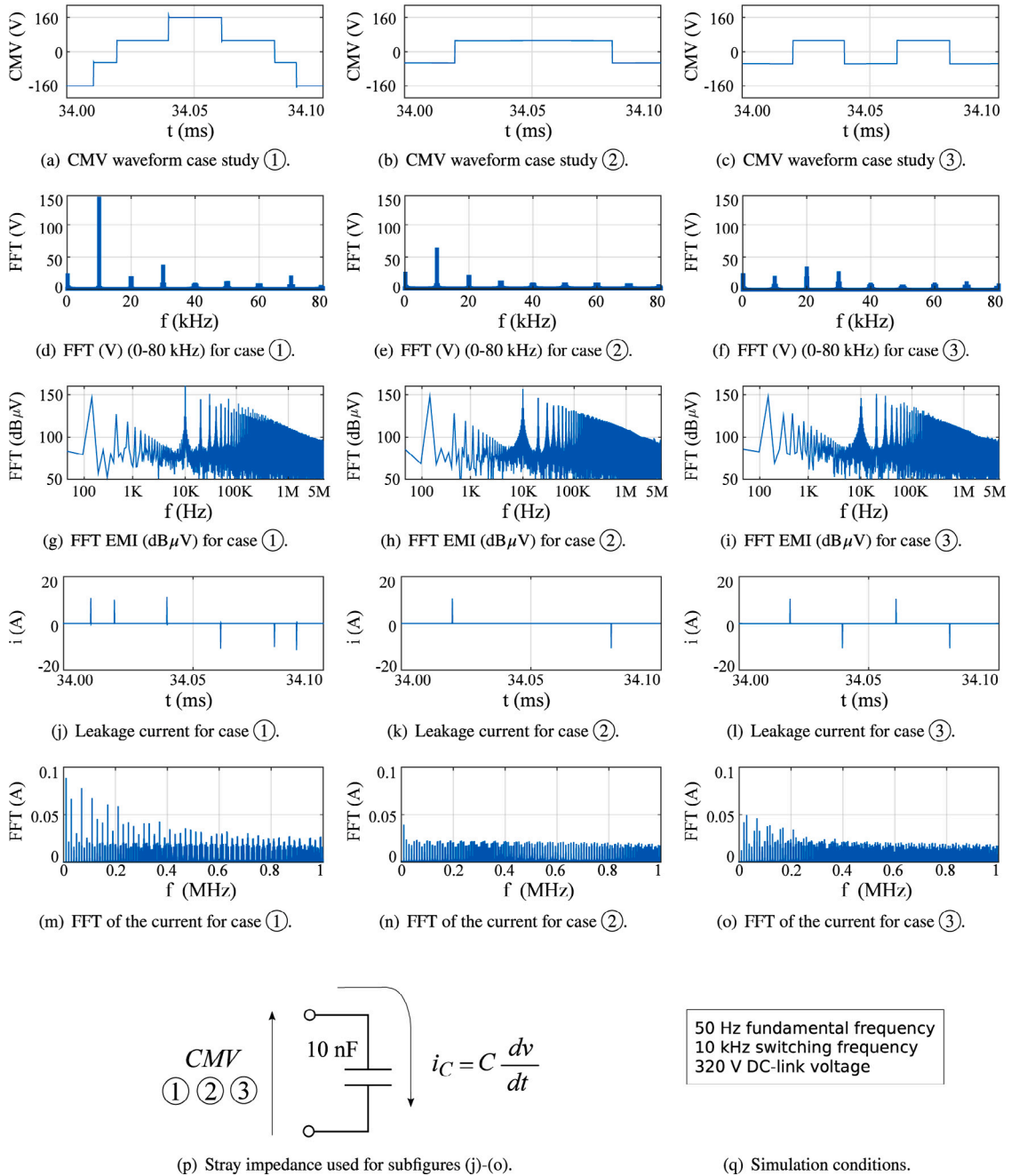


Fig. 4. Representation of three case studies (patterns) of the CMV waveform using SV-PWM, both in time and frequency domain: left (VSI Conventional Converter), middle (H8D2 Converter), right (VSIZVR-D1 Converter) [28].

This is achieved with pattern (3). Although it has two more voltage variations (Figs. 4(b) and 4(c)), it distributes the harmonics with less amplitude in a greater number of frequencies (Figs. 4(e) and 4(f)). Consequently, if EMI protections are used, they should be dimensioned for lower signal amplitudes.

On the other hand, to analyse the effect of a certain CMV-derived current, a machine stray capacitance of 10 nF has been considered (Fig. 4(p)) to carry out simulations for the three CMV patterns. The time domain currents are shown in Figs. 4(j)–4(l), while frequency responses are depicted in Figs. 4(m)–4(o). Considering (3), where $z(i)$ represents the i th harmonic of the leakage current, the pattern (2) shows a better performance than (3) (Table 3). The worst results are obtained when applying pattern (1), which is the most common CMV waveform in

Table 3
Harmonic energies of normalized CMV and leakage currents for the three case studies of Fig. 4.

Pattern	Normalized energy of the CMV (2)	Energy of leakage currents (3)
①	0.92	1.38
②	0.22	0.45
③	0.20	0.91

Note: ✓ indicates the best alternative.

three-phase inverters.

$$E(i_C) \approx \sum_{i=1}^{\infty} [z(i)]^2. \quad (3)$$

Consequently, for each particular application, it is necessary to consider which is the best mitigation alternative depending which CMV issue is prioritized, i.e., EMI, leakage currents, etc. Therefore, in order to facilitate the analysis of CMV and the mitigation solutions, the utilization of the following figures-of-merit is proposed in this work:

1. $\Delta_p \in [0, 1]$ - Peak-to-peak value of waveform, relative to V_{DC} .
2. $\Delta_S \in [0, \Delta_p]$ - Height of largest CMV step, also relative to V_{DC} .
3. N_L - Number of different levels per T_{sw} .
4. N_T - Number of transitions (step shifts) per T_{sw} .

These figures-of-merit are useful to understand the CMV problem. Depending on the application, the engineer who designs the motor drive must make the most convenient decisions. What is clear is that reducing the amplitude of the CMV is important, while also minimizing the number of variations (dv/dt) and the dv/dt value. Therefore, these and other CMV-related particularities are best captured by the previous 'the lower the better' figures-of-merit [30], which are helpful in understanding and comparing the CMV alternative waveforms to be presented in this work. For example, in a conventional three-phase two-level VSI, SV-PWM is characterized by $\Delta_p = 1$, $\Delta_S = 1/3$, $N_L = 4$, and $N_T = 6$ (Fig. 2), which are rather poor values, as indicated in [30]. Thus, in general, it will be interesting to find a balance between the reductions of each figure-of-merit to achieve a CMV pattern that improves all the problems involved in electric motor drives.

Although hardware and modulation solutions can be applied to two-level three-phase VSIs, multiphase converter topologies can be considered for CMV mitigation purposes thanks to their additional degrees of freedom. This topic will be covered in the next sections, where the most relevant multiphase converter topologies and modulation techniques in this field are reviewed (Sections 3 and 4, respectively).

3. Common-mode voltage in multiphase inverter topologies

Fig. 5 summarizes the most relevant multiphase topologies. Although such topologies⁶ are not directly intended for CMV mitigation, their additional degrees of freedom can be exploited for that purpose. By implementing advanced modulation algorithms, the CMV can be effectively reduced, or even eliminated. Therefore, it is interesting to review the possibilities offered by these power conversion solutions. In this sense, since each vector has an associated switching state, the relationship between SV-PWM vectors and the switching states of each converter is straightforward, thus helping to better understand the CMV differences between converter architectures.

3.1. Multiphase inverters feeding a star-connected load

Fig. 5(a) shows an m -phase power converter supplying a star-connected electric machine with a single neutral point.⁷ This popular configuration is usually constituted by an odd number of phases. This is because, for example, a five-phase star-connected system has the same

⁶ It is worth mentioning that the number of phases of the load (generally an electric machine) is commonly considered to classify whether an electric drive is a multiphase system or not. For example, star connected m -phase (Fig. 5(a), $m > 3$) [75,76], dual three-phase (Fig. 5(c)) [50,77,78], and open winding m -phase (Fig. 5(d)) [79] drive configurations fall into this category. However, as this work also focuses on power converters, any power converter with more than three legs has been considered as a multiphase system. This way, three-phase four-leg configurations with access to the neutral point of the machine [80] (Fig. 5(b)) and open-end three-phase converters [81] (Fig. 5(d)) have been also categorized as multiphase systems. Therefore, as in the other topologies, their concepts related to CMV can be extended to a converter with a greater number of phases.

⁷ Although there is no physical limitation on the number of phases that can be added to the converter, research is mainly focused on five-phase converters.

amount of degrees of freedom (four independently controllable variables) as a six-phase one. In contrast, the latter has two non-controllable homopolar components [82].

Star-connected multiphase electric drives exhibit various interesting features. On the one hand, when the machine stator has concentrated windings (back-EMF with triplen harmonics), it is possible to take advantage of the additional degrees of freedom and regulate the third harmonic current component. This way, torque production can be enhanced by approximately 15% [54,83], and therefore a better power density is achieved. Also, the additional control degrees of freedom of the star-connected multiphase drives can be exploited when one or various phases have open-circuit faults. This gives a low torque ripple with the remaining healthy phases and leads to a pseudo-optimum operation, which also provides limp-home operation capabilities [75, 84,85]. In such cases, it is necessary to over-dimension the electric machine and the power converter, as unbalanced currents circulate through the remaining phases during fault-tolerant operation. Thus, star-connected multiphase systems are considered promising topologies for critical applications where fault tolerance and power density are key features [48,49].

The number of available switching states in this multiphase converter is 2^m , which is the same as the number of available space vectors to synthesize the reference fundamental output voltage vector and the triplen harmonics.⁸ In this sense, Fig. 6 shows the SV representation of a five-phase system in the $\alpha\beta$ - and xy -planes. These subspaces are obtained by applying the following amplitude-invariant Clarke transformation to the per-phase phase-to-neutral output voltages for all permitted switching configurations of the inverter [60]:

$$\begin{bmatrix} v_\alpha \\ v_\beta \\ v_x \\ v_y \\ v_0 \end{bmatrix} = \frac{2}{5} \begin{bmatrix} 1 & \cos(2\pi/5) & \cos(4\pi/5) & \cos(6\pi/5) & \cos(8\pi/5) \\ 0 & \sin(2\pi/5) & \sin(4\pi/5) & \sin(6\pi/5) & \sin(8\pi/5) \\ 1 & \cos(4\pi/5) & \cos(8\pi/5) & \cos(12\pi/5) & \cos(16\pi/5) \\ 0 & \sin(4\pi/5) & \sin(8\pi/5) & \sin(12\pi/5) & \sin(16\pi/5) \\ \frac{1}{2} & \frac{1}{2} & \frac{1}{2} & \frac{1}{2} & \frac{1}{2} \end{bmatrix} \begin{bmatrix} v_1 \\ v_2 \\ v_3 \\ v_4 \\ v_5 \end{bmatrix}. \quad (4)$$

The application of (4) projects the $h = 5(l-1) \pm 1$ voltage harmonic components into the $\alpha\beta$ -plane, while $h = 5(l-1) \pm 3$ harmonics are projected into the xy -plane, where $l = 1, 3, 5, \dots$ [60].⁹

Likewise, the CMV levels produced by each SV or switching state are obtained as:

$$v_{CM}(t) = \frac{1}{m} \sum_{i=1}^m v_{i0}, \quad (5)$$

where m is the number of phases and v_{i0} is the i^{th} inverter output phase-to-ground voltage; see Fig. 5(a). Table 4 summarizes the CMV values obtained when applying a given vector. These values are present in the CMV waveform when the SV-PWM modulation technique is used [60], and thus the CMV related figures-of-merit N_T and N_L increase with the number of phases, while Δ_S decreases. However, it is possible to implement modulation alternatives for these converter structures targeting CMV mitigation [86,87]. These modulation techniques will be comprehensively reviewed in Section 4.

⁸ This makes that SV-PWM implementation more complex than in three-phase systems. For this reason, CB-PWM techniques are generally preferred by the industry in this type of power converters.

⁹ It must be pointed out that infinitely many possible Clarke transformations can be defined. However, this is one of the most convenient, as it maps the fundamental and third harmonic components (most significant torque contributors) into two independent bi-dimensional planes, decoupling their control.

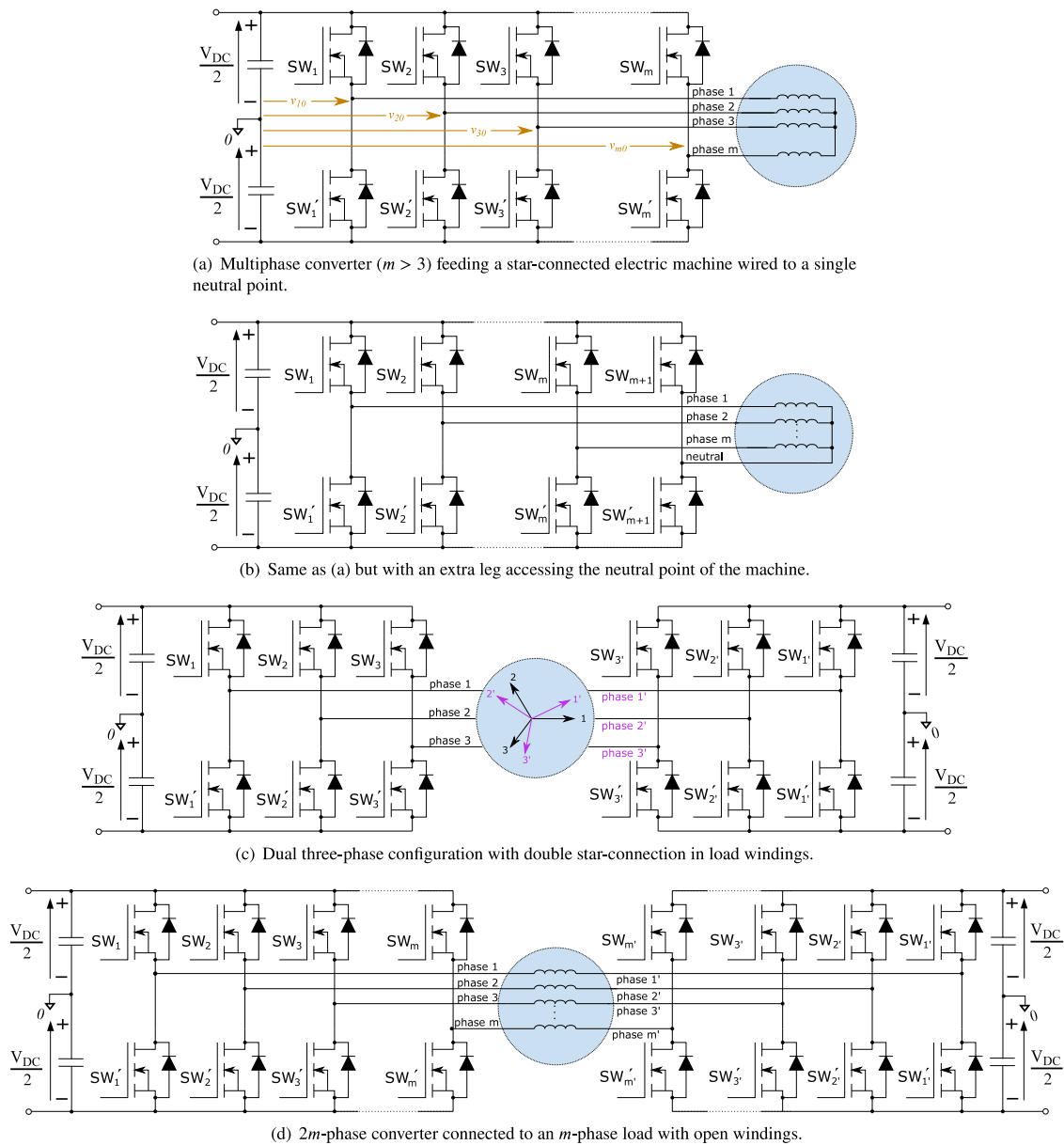


Fig. 5. Most widely used multiphase power conversion topologies [73].

3.2. Multiphase ($m + 1$)-leg converters

Fig. 5(b) shows this multiphase alternative, which incorporates an extra leg to an m -phase inverter ($m \geq 3$), thus providing access to the neutral point of the load. Particularly, the three-phase four-leg configuration has been mostly investigated¹⁰ in applications such as photovoltaic systems [90], uninterruptible power supplies [80], and grid-connected applications [91], as well as Electric Machine Drive Systems (EMDS)¹¹ [92–94].

This architecture allows controlling the voltage value of the neutral point. The resulting additional degree of freedom can be used to control unbalanced loads [95,96]. However, this configuration has mainly been exploited to provide fault tolerance to three-phase drive systems [93,

94]. When a single-phase open-circuit fault occurs, the two remaining healthy phase currents of the inverter branches are increased by $\sqrt{3}$ in magnitude and regulated with a relative phase-shift of 60° , thus maintaining a uniform rotational magneto-motive force and providing a low torque ripple [94].

In a three-phase four-leg converter, a three-dimensional SV representation (Fig. 7) replaces the traditional bi-dimensional $\alpha\beta$ -plane of a three-phase system [97,98]. The third dimension is given by the homopolar component which sorts space vectors into different layers of the γ -axis [97]. The resulting three-dimensional vector space becomes more complex as the number of phases of the converter increases. Nonetheless, PWM techniques have also been proposed that allow controlling the fourth leg independently from the phases [89,99].

Again, the CMV is defined by (5) in m -phase ($m+1$)-leg converters, but in this particular case, m represents the total number of legs instead of the number of phases. For example, when 3D SV-PWM is used to control a three-phase four-leg converter, $0, \pm V_{DC}/4$ and $\pm V_{DC}/2$ CMV levels (Table 5) are obtained [90]. However, the extra degree

¹⁰ The five-phase six-leg configuration has been recently investigated for power amplifiers in [88,89]. However, it is uncommon to find topologies having more than four legs.

¹¹ Note that machines with special designs providing physical access to the neutral point are required in these electric drives.

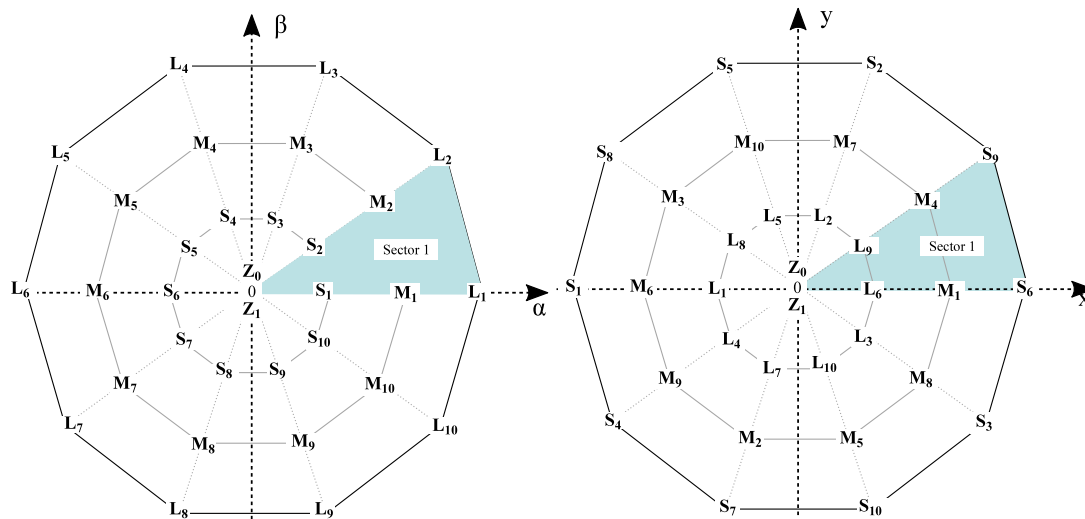


Fig. 6. Zero (Z), small (S), medium (M), and large (L) vector placement in the fundamental harmonic ($\alpha\beta$) and triplen harmonics (xy) planes for a five-phase power inverter.

Table 4
CMV levels in a five-phase inverter, depending on the applied vector (see also Fig. 6).

Five-phase inverter		
Vector type	Voltage vectors (switching state)	CMV level [V]
Zero	Z_0 (00000)	$-V_{DC}/2$
Medium	M_1 (10000), M_3 (01000), M_5 (00100), M_7 (00010), M_9 (00001)	$-3V_{DC}/10$
Large	L_2 (11000), L_4 (01100), L_6 (00110), L_8 (00011), L_{10} (10001)	$-V_{DC}/10$
Small	S_1 (01001), S_3 (10100), S_5 (01010), S_7 (00101), S_9 (10010) S_2 (11010), S_4 (01101), S_6 (10110), S_8 (01011), S_{10} (10101)	$V_{DC}/10$
Large	L_1 (11001), L_3 (11100), L_5 (01110), L_7 (00111), L_9 (10011)	$V_{DC}/10$
Medium	M_2 (11101), M_4 (11110), M_6 (01111), M_8 (10111), M_{10} (11011)	$3V_{DC}/10$
Zero	Z_1 (11111)	$V_{DC}/2$

Table 5
CMV levels of three-phase four-leg converter according to the applied vectors (see Fig. 7).

Three-phase four-leg inverter		
Vector type	Voltage vectors (switching state)	CMV level [V]
Zero	P_0'' (0000)	$-V_{DC}/2$
Zero lower	P_0' (0001)	$-V_{DC}/4$
Odd upper	P_1'' (1000), P_3'' (0100), P_5'' (0010)	0
Even upper	P_2'' (1100), P_4'' (0110), P_6'' (1010)	0
Odd lower	P_1' (1001), P_3' (0101), P_5' (0011)	0
Even lower	P_2' (1101), P_4' (0111), P_6' (1011)	$V_{DC}/4$
Zero upper	P_7'' (1110)	$V_{DC}/4$
Zero	P_7' (1111)	$V_{DC}/2$

of freedom provided by the additional leg allows developing PWM techniques that reduce the CMV [100,101].

3.3. Multiple three-phase drive configurations

Fig. 5(c) presents the dual three-phase configuration. According to the most recent literature, this architecture is probably the most

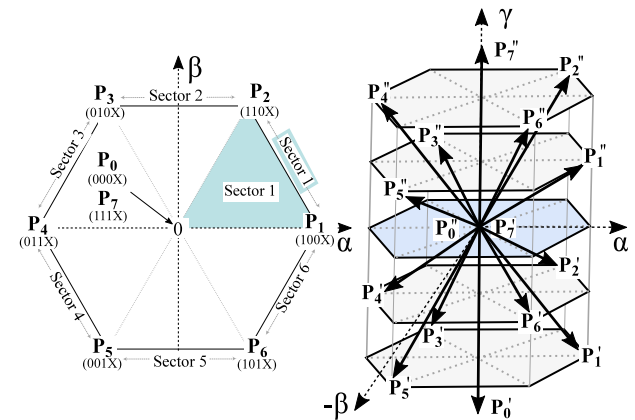


Fig. 7. Space vectors of a three-phase four-leg power converter.

popular one among all the multiphase solutions [78,102,103]. Note that although virtually any number of three-phase sets could be theoretically implemented,¹² it is uncommon to find solutions with more than two phase sets.

Dual three-phase configurations are preferred as (i) they represent a good trade-off between performance and complexity, (ii) migration from three-phase to dual three-phase technologies is straightforward [50], and (iii) this configuration exhibits an excellent fault tolerant performance [78,102,105,106], thus making them attractive for safety-critical applications.

In this configuration, two symmetrically (0° or 60°) or asymmetrically (30°) shifted three-phase winding sets with independent and isolated neutral points are fed by (i) two separated three-phase inverters (including independent three-phase controllers) [107], or by (ii) a single six-phase inverter (which control considers all the cross-coupling effects by using convenient vector transformations) [50]. In this context, although it is easier to manufacture machines in a symmetrical winding arrangement, the asymmetrical winding distribution is preferred because of the cancellation of the sixth torque harmonic, and lower cross coupling effects between winding sets [108].

¹² There are few works that investigate triple three-phase machines or with more than two phase sets. An example is [104] that investigates a fault tolerant control technique for a triple three-phase surface permanent magnet machine.

Table 6

CMV of a dual three-phase converter according to the obtained per phase voltage level (see Fig. 8).

Dual three-phase inverter	
Voltage vector combinations	CMV level [V]
$[V_0, V_0']$	$-V_{DC}/2$
$[V_0, V_1'] [V_0, V_3'] [V_0, V_5']$ $[V_1, V_0'] [V_3, V_0'] [V_5, V_0']$	$-V_{DC}/3$
$[V_0, V_2'] [V_0, V_4'] [V_0, V_6']$ $[V_1, V_1'] [V_1, V_3'] [V_1, V_5']$ $[V_3, V_1'] [V_3, V_3'] [V_3, V_5']$ $[V_5, V_1'] [V_5, V_3'] [V_5, V_5']$ $[V_2, V_0'] [V_4, V_0'] [V_6, V_0']$	$-V_{DC}/6$
$[V_1, V_2'] [V_1, V_4'] [V_1, V_6']$ $[V_3, V_2'] [V_3, V_4'] [V_3, V_6']$ $[V_5, V_2'] [V_5, V_4'] [V_5, V_6']$ $[V_2, V_1'] [V_4, V_1'] [V_6, V_1']$ $[V_2, V_3'] [V_4, V_3'] [V_6, V_3']$ $[V_2, V_5'] [V_4, V_5'] [V_6, V_5']$ $[V_0, V_7'] [V_7, V_0']$	0
$[V_1, V_7'] [V_3, V_7'] [V_5, V_7']$ $[V_2, V_2'] [V_2, V_4'] [V_2, V_6']$ $[V_4, V_2'] [V_4, V_4'] [V_4, V_6']$ $[V_6, V_2'] [V_6, V_4'] [V_6, V_6']$ $[V_7, V_1'] [V_7, V_3'] [V_7, V_5']$	$V_{DC}/6$
$[V_2, V_7'] [V_4, V_7'] [V_6, V_7']$ $[V_7, V_2'] [V_7, V_4'] [V_7, V_6']$	$V_{DC}/3$
$[V_7, V_7']$	$V_{DC}/2$

Switching states are shown in Table 2.

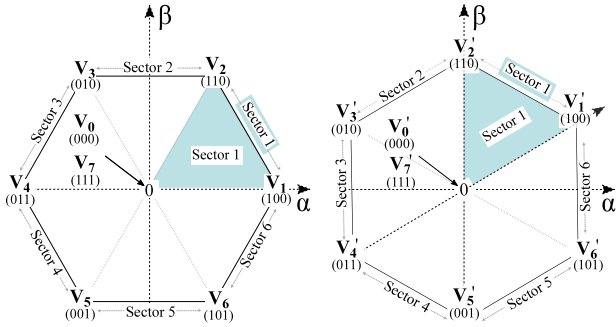


Fig. 8. Representation of the two $\alpha\beta$ planes of the dual three-phase inverter.

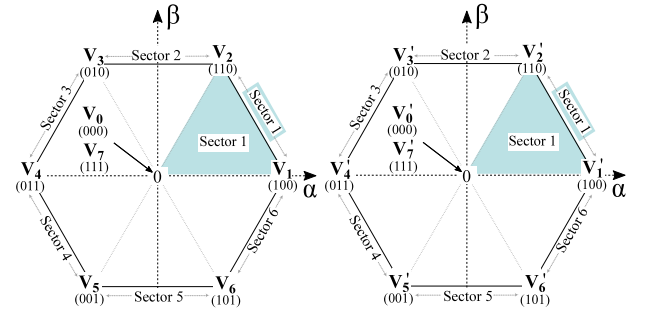
Regarding the modulation, once the controller determines the $\alpha\beta$ reference voltages to be synthesized in each winding set (with their corresponding phase shift), two independent three-phase SV-PWMs (or CB-PWMs) can be applied (see Fig. 8). In this context, CMV in dual three-phase systems can be defined from the individual v_{CM1} and v_{CM2} CMVs produced by each inverter [64,108]:

$$v_{CM}(t) = \frac{1}{2} [v_{CM1}(t) + v_{CM2}(t)] = \frac{1}{6} \left[\sum_{i=1}^3 v_{i0}(t) + \sum_{j=1}^3 v_{j0}(t) \right], \quad (6)$$

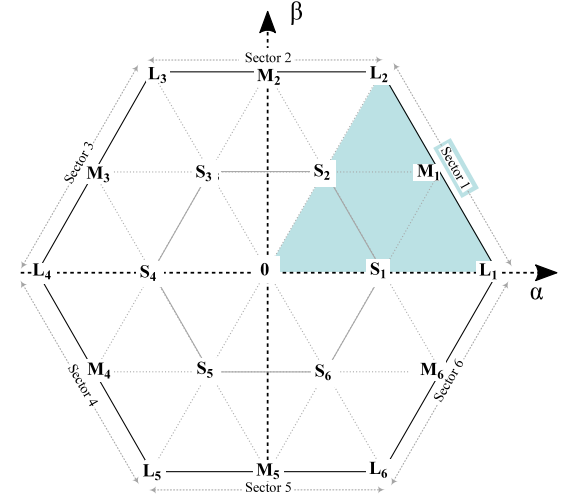
where v_{i0} and v_{j0} are the per-phase phase-to-ground voltages of the two inverters, respectively, and indexes i and $j = 1, 2, 3$. This leads to the CMV levels summarized in Table 6. Note that each vector pair shown in Table 6 indicates the vector combination applied by both inverters. As in other multiphase systems, this CMV can be mitigated by applying several modulation algorithms [64,108–110].

3.4. Open-end multiphase inverters

Finally, Fig. 5(d) shows an open-end inverter for a given load number of phases [111–113], which is the most complex of all the multiphase solutions, as each end is connected to an m -phase inverter



(a) Space-vector distribution of each individual subspace of VSI.



(b) Space vectors resulting from combining the two subspaces.

Fig. 9. Open-end three-phase inverter space-vector diagram (relationship between space vectors shown in Table 7).

(Fig. 5(d)). Thus, the per-phase switch count of this topology is the highest one, doubling the one of an equivalent star-connected multiphase system. In this particular configuration, it is possible to have two differentiated inverters with independent power supplies [114] or, which is more common, with both inverters sharing a single DC supply (an H-bridge per load phase) [76].

Despite the additional complexity, the extra degrees of freedom provide redundancy in the inverter states [115], so this converter architecture can generate the same output voltage levels as a multilevel converter [116]. All these redundancies can be used to develop PWM techniques for low-order harmonics elimination, or also to reduce the CMV [81,117]. For example, 64 vector combinations are possible in three-phase open-end inverters when the two vector subspaces shown in Fig. 9(a) are combined. Indeed, this combination results in the vector space of a three-level converter shown in Fig. 9(b), where several of the vector combinations produce the same voltage levels.

Regarding the CMV, two contributions, i.e., average (v_{CMav}) and differential (v_{CMdiff}), are considered from the individual v_{CM1} and v_{CM2} voltages generated by each end inverter [118]. A generalization for an m -phase system results in

$$v_{CMav}(t) = \frac{1}{2} [v_{CM1}(t) + v_{CM2}(t)] = \frac{1}{2m} \left[\sum_{i=1}^m v_{i0}(t) + \sum_{j=1}^m v_{j0}(t) \right], \quad (7)$$

and

$$v_{CMdiff}(t) = v_{CM1}(t) - v_{CM2}(t) = \frac{1}{m} \left[\sum_{i=1}^m v_{i0}(t) - \sum_{j=1}^m v_{j0}(t) \right], \quad (8)$$

where m is the number of load phases. It is important to highlight that the differential CMV generates circulating currents, whereas the

average CMV affects EMI [118,119]. As an example, Table 7 lists all the CMV levels of an open-end three-phase system. Again, vector pairs represent the vector combinations applied at both end inverters. Therefore, the same average CMV levels as in a dual-three phase system are obtained. Again, CMV can be mitigated by applying specific modulation techniques [53,115,119–121].

As a summary, Table 8 shows the most relevant CMV and hardware-related features of the four multiphase architectures dealt with in this section, including the advantages and drawbacks of each approach. For all these architectures, the figures-of-merit previously defined in Section 2 can be generalized depending on the phase-number (leg-number), as shown in Fig. 10. For example, Fig. 10(b) represents the figures-of-merit of the three-phase four-leg converter with access to the neutral point of the machine; Fig. 10(c) considers the five-phase converter with star connection; and Fig. 10(d) includes the five-phase six-leg converter, as well as the dual three-phase configuration and the configuration with two converters connected to a three-phase load with open windings. In conclusion, Fig. 10 shows how increasing the number of phases of a converter affects the CMV. As the number of phases (legs) is increased, Δ_S decreases while N_L and N_T increase. On the contrary, Δ_P remains invariant as, without applying an specific modulation technique, multiphase converters themselves do not reduce the CMV, as it happens in three-phase converters [30]. In this regard, the most important modulation techniques proposed to reduce CMV in multiphase converters are reviewed below.

4. Advanced modulation techniques for common-mode voltage reduction in star-connected multiphase systems

Among all the multiphase converter alternatives reviewed in the previous section, and how the CMV affects all of them in different way, it can be concluded that m -phase inverters feeding star-connected loads provide the best trade-off between control complexity and CMV reduction potential. In this line, the scientific literature shows how five-phase configurations have been mainly investigated, in terms of modulation, for CMV mitigation [68,86,122,123]. Therefore, this work mainly analyses the modulation techniques for this converter topology. On the other hand, since modulation techniques based on SV-PWM provide a higher level of abstraction than carrier-based (CB) ones with regard to CMV, it has been decided to set aside CB modulation techniques that are proposed to reduce the CMV. Thus, once the impact of traditional SV-PWM is presented for five-phase converters, this section looks into the most relevant modulation families that can be used in such systems. In this sense, following the same modulation categories that were reviewed in [30] for three-phase converters, the SV-based modulations for CMV mitigation in multiphase inverters can be classified as:

- Discontinuous modulation (D-PWM) techniques. Their main goal is to reduce the number of commutations per switching period (T_{SW}), thus lowering power losses [125,126]. Although these algorithms are not directly intended for CMV reduction, they provide some kind of mitigation. Thus, they are worth being considered in the CMV context.
- Reduced CMV PWM (RCMV-PWM) techniques. These modulations are directly intended for CMV mitigation, providing significant CMV reduction. This broad family includes the following sub-families: (a) Active zero-state PWM (AZS-PWM) [74,127], (b) Remote-state PWM (RS-PWM) [128,129] and (c) Near-state PWM (NS-PWM) [130,131].
- Other modulation techniques for CMV elimination. Furthermore, other modulation techniques as the ‘Constant CMV’ PWM (CCMV-PWM) have been proposed in three-phase converters. This latter technique is able to completely eliminate the CMV variations in three-phase converters when combined with a special converter topology, which includes additional hardware elements [25,28].

Table 7

CMV of an open-end three-phase inverter according to the per-phase voltage level obtained (see Fig. 9).

Open-end three-phase inverter				
Vector type	Voltage vector combinations ^a	Multilevel vector	Average CMV [V] ^b	Differential CMV [V] ^c
Zero	$[V_0, V_0']$	0	$-V_{DC}/2$	0
Small	$[V_0, V_5'] [V_0, V_1'] [V_0, V_3']$	$S_2 S_4 S_6$	$-V_{DC}/3$	$-V_{DC}/3$
	$[V_1, V_0'] [V_3, V_0'] [V_5, V_0']$	$S_1 S_3 S_5$	$-V_{DC}/3$	$V_{DC}/3$
	$[V_0, V_4'] [V_0, V_6'] [V_0, V_2']$	$S_1 S_3 S_5$	$-V_{DC}/6$	$-2V_{DC}/3$
Zero	$[V_1, V_1'] [V_3, V_3'] [V_5, V_5']$	0 0 0	$-V_{DC}/6$	0
Medium	$[V_1, V_5'] [V_3, V_5'] [V_3, V_1']$	$M_1 M_2 M_3$		
	$[V_5, V_1'] [V_5, V_3'] [V_1, V_3']$	$M_4 M_5 M_6$		
Small	$[V_2, V_0'] [V_4, V_0'] [V_6, V_0']$	$S_2 S_4 S_6$	$-V_{DC}/6$	$2V_{DC}/3$
Zero	$[V_0, V_7']$	0	0	$-V_{DC}$
Small	$[V_1, V_6'] [V_5, V_6'] [V_1, V_2']$	$S_2 S_4 S_6$	0	$-V_{DC}/3$
	$[V_3, V_4'] [V_3, V_2'] [V_5, V_4']$	$S_2 S_4 S_6$		
Large	$[V_1, V_4'] [V_3, V_6'] [V_5, V_2']$	$L_1 L_3 L_5$	0	$V_{DC}/3$
	$[V_2, V_5'] [V_4, V_1'] [V_6, V_3']$	$L_2 L_4 L_6$		
Small	$[V_2, V_3'] [V_2, V_1'] [V_4, V_3']$	$S_1 S_3 S_5$	0	$V_{DC}/3$
	$[V_6, V_5'] [V_4, V_5'] [V_6, V_1']$	$S_1 S_3 S_5$		
Zero	$[V_7, V_0']$	0	0	V_{DC}
Small	$[V_1, V_7'] [V_3, V_7'] [V_5, V_7']$	$S_1 S_3 S_5$	$V_{DC}/6$	$-2V_{DC}/3$
Zero	$[V_2, V_2'] [V_4, V_4'] [V_6, V_6']$	0 0 0	$V_{DC}/6$	0
Medium	$[V_2, V_4'] [V_2, V_6'] [V_4, V_6']$	$M_1 M_2 M_3$	$V_{DC}/6$	0
	$[V_4, V_2'] [V_6, V_2'] [V_6, V_4']$	$M_4 M_5 M_6$		
Small	$[V_7, V_5'] [V_7, V_1'] [V_7, V_3']$	$S_2 S_4 S_6$	$V_{DC}/6$	$2V_{DC}/3$
	$[V_2, V_7'] [V_4, V_7'] [V_6, V_7']$	$S_2 S_4 S_6$	$V_{DC}/3$	$-V_{DC}/3$
	$[V_7, V_4'] [V_7, V_6'] [V_7, V_2']$	$S_1 S_3 S_5$	$V_{DC}/3$	$V_{DC}/3$
Zero	$[V_7, V_7']$	0	$V_{DC}/2$	0

^aSwitching states are shown in Table 2.

^bDifferential CMV is calculated as (8).

^cAverage CMV is calculated as (7).

Following this approach, Section 4.4 is reserved here to review other techniques that serve a similar purpose in the multiphase scenario and are not classified within the two previous groups. In addition, other modulation methods are analysed to reduce CMV in closed-loop, which are based on the model predictive control (MPC) [132], such as finite set predictive control [122].

In the following analysis, emphasis is placed on the synthesis of the reference vector (V_{ref}), the linear range (LR), and the produced CMV.¹³ As previously mentioned, in all cases, the space vector (SV) approach has been chosen as it provides a higher abstraction level, which makes it easier to relate the CMV figures-of-merit (Section 2) with the vector sequence of each modulation technique.¹⁴

4.1. Traditional SV-PWM for five-phase inverters feeding a star-connected load

By choosing a convenient Clarke transformation, the output currents and voltages of an m -phase star-connected inverter can be represented

¹³ The synthesis of the reference vector refers to how the inverter output voltages are synthesized, whereas synthesized and the linear range specifies the percentage of utilization of the DC bus.

¹⁴ The previous paper by the authors [30] explains that the CMV waveform produced by a given modulation algorithm does not depend on whether it is implemented following a CB or SV-based approach, since the same CMV waveform can be obtained with both approaches.

Table 8
Main multiphase inverters and their relationship with the CMV^a.

	Multiphase feeding a star-connected load		m -phase ($m + 1$)-leg converters		Multiple three-phase converters with shifted three-phase windings	Converter connected to a load with open windings		
	Five-phase	m -phase	Four-leg three-phase	Six-leg five-phase	Dual three-phase	Open-end three-phase	Open-end five-phase	
	Fig. 5(a)		Fig. 5(b)		Fig. 5(c)	Fig. 5(d)		
Hardware ^b	• Switches ^c	10	2 m	8	12	12	12	20
	• Diodes	0	0	0	0	0	0	0
	• DC bus capacitors ^e	1	1	1	1	1 or 2	1 or 2	1 or 2
	• Extra capacitors	0	0	0	0	0	0	0
	• Inductors	0	0	0	0	0	0	0
	• Voltage sources	1	1	1	1	1 or 2	1 or 2	1 or 2
CMV-related data ^d	• CMV waveform in five-phase inverter and generalized to m -phase inverter							
	• CMV figures-of-merit	Δ_p	1	1	1	1	1	1
	Δ_S	1/5	1/ m	1/4	1/6	1/6	1/6	1/10
	N_L	6	$m + 1$	5	7	7	7	11
	N_T	10	2 m	8	12	12	12	20
Pros and cons	• Advantages	<ul style="list-style-type: none"> • Fault tolerance under various open-circuit faults • Current harmonic injection capabilities • Degrees of freedom vs. phase number relationship 		<ul style="list-style-type: none"> • Provides fault tolerance even for three-phase loads • One more degree of freedom • Neutral point voltage control 		<ul style="list-style-type: none"> • Fault tolerance under open and short circuit faults • Fault tolerance under power supply faults^f • Easy migration from three-phase technologies is possible 		<ul style="list-style-type: none"> • Fault tolerance under open and short circuit faults • Flexibility due to high number of switching states • Ability to produce multilevel output
	• Disadvantages	<ul style="list-style-type: none"> • Sensitive to power supply faults • Complex modulation scheme 		<ul style="list-style-type: none"> • Sensitive to power supply faults • Access to machine neutral point required • Additional devices by the ($m + 1$)-leg 		<ul style="list-style-type: none"> • Difficulty of expanding to converters having more than three-phase^g 		<ul style="list-style-type: none"> • High switch count • Complex modulation scheme
References	[60,86,87,124]		[89,90,97,98,100]		[78,105,106,108]		[111,115,118–120]	

Table notes:

^aAs this work focuses on power converters, any power converter with more than three legs has been considered as a multiphase system (three-phase four-leg (Fig. 5(b)) and the open-end three-phase (Fig. 5(d)) converters have been categorized as multiphase systems).

^bAlthough here some elements are 0 in other topologies, such as multilevel or other three-phase two-level topologies with more devices, this does not happen.

^cSwitches (with freewheeling diodes).

^dThe CMV can be extended to ($m + 1$) levels (bounded between $\pm V_{dc}/2$) in steps of V_{dc}/m value considering m as the total number of legs, and not as the total number of phases (these phases referred to the load). In addition, it is assumed that all CMV values appear during T_{sw} , which does not always happen.

^eMinimum number of DC-bus capacitors, withstanding the same voltage.

^fOnly when separated supplies are provided.

^gDual five-phase or higher solutions have not been found in the relevant literature.

in $(m-1)/2$ two-dimensional orthogonal planes and in a single homopolar component [86]. As the homopolar component can be neglected when the machine has a star-connected winding with an isolated neutral point [133], an $m - 1$ dimensional representation is obtained. Such Clarke transformation has been previously defined in (4) for a five-phase system. The projection of the 32 allowed converter switching states leads to the following vector distribution in the resulting $\alpha\beta$ (fundamental component) and xy (triplen harmonics) planes:

- 30 active vectors, which can be classified as large ($\mathbf{L}_1 - \mathbf{L}_{10}$), medium ($\mathbf{M}_1 - \mathbf{M}_{10}$) and small ($\mathbf{S}_1 - \mathbf{S}_{10}$), according to their magnitude; see Fig. 6.
- Two zero vectors, \mathbf{Z}_0 and \mathbf{Z}_1 ; see also Fig. 6.

A simple extension of the three-phase SV modulation, named 2L-SV-PWM, consists on using the two large active vectors neighbouring the reference vector and the two zero vectors to synthesize \mathbf{V}_{ref} . Although simple, this approach generates significant low order output voltage

harmonics due to the resulting non-zero voltage vector in the xy -plane [134,135]. Such low-order harmonics can be eliminated by using the additional degrees of freedom of the multiphase system. By using four active vectors, and conveniently determining their application times, the voltage vector projection in the xy -plane is, on average, zero [136,137].¹⁵ The two SV-PWM variants that are mostly used are [134,137]:

- The 4L-SV-PWM technique, which uses four large vectors neighbouring the reference and the two zero vectors.
- The 2L2M-SV-PWM technique, where two medium and two large vectors are used in addition to both zero vectors. To eliminate the third harmonic content, large vectors are applied during a

¹⁵ When the load windings follow a sinusoidal distribution, a sinusoidal output current is generated. If windings follow a concentrated distribution, the third harmonic can be useful to enhance the torque production. In such a case, it is necessary that the sum of the vectors in the xy -plane is not zero [135].

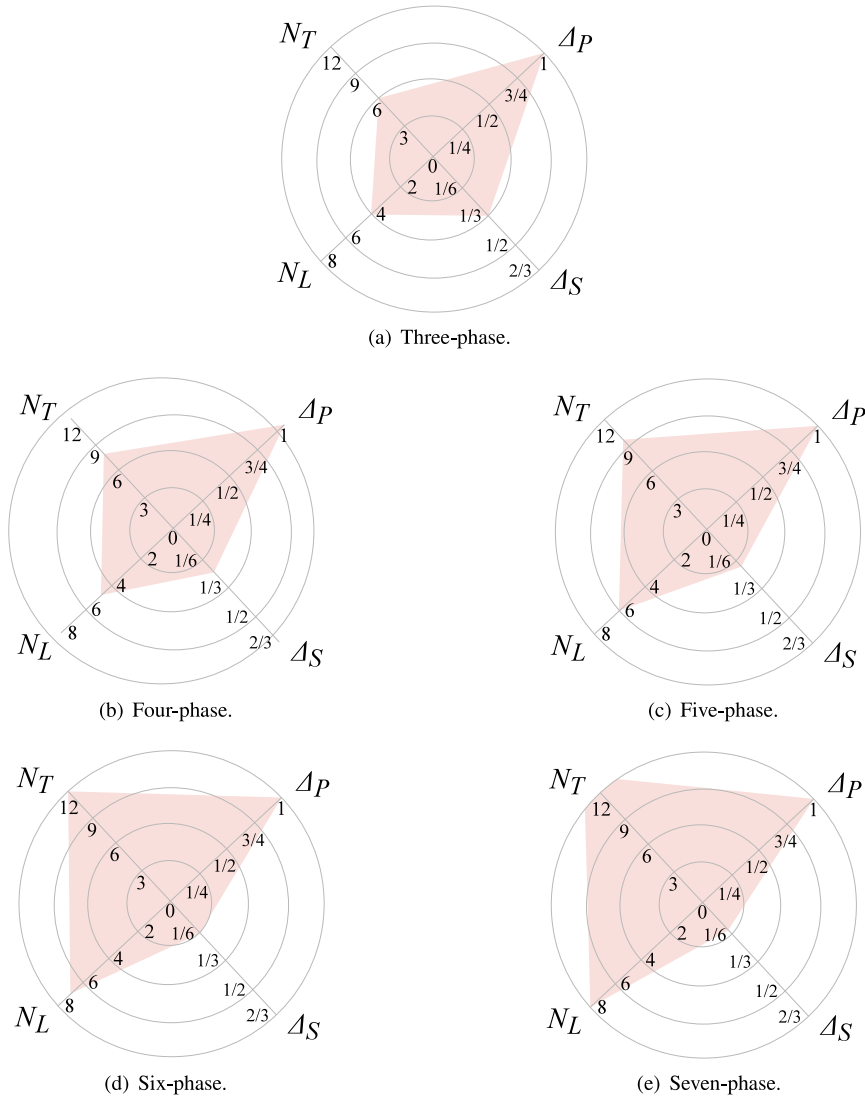


Fig. 10. Figures-of-merit in multiphase architectures vs. phase-number (leg-number).

61.8 % of each active vector application-time, while medium vectors are applied a 38.2 % [134]. As an illustrative example, Fig. 11(a) shows the applied vectors for 2L2M-SV-PWM when \mathbf{V}_{ref} lies in sector 1.

Regarding the LR, if only two large vectors are used (2L-SV-PWM technique), the maximum synthesizable output voltage vector magnitude is $0.6155 V_{DC}$, and the amplitude modulation index $M_a \in [0, 1.231]$ (Fig. 11(b)). Conversely, both 2L2M-SV-PWM and 4L-SV-PWM techniques achieve a lower utilization of the DC bus voltage, with the maximum synthesizable vector magnitude equalling $0.5257 V_{DC}$. Consequently, in both cases $M_a \in [0, 1.051]$ (Fig. 11(b)) [126,137].

Finally and considering (5), Fig. 11(c) shows the CMV waveform produced when \mathbf{V}_{ref} lies in sector 1 and the 2L2M-SV-PWM pattern is applied (the corresponding switching states are shown in Fig. 11(d), and CMV levels are summarized in Table 4). This represents the worst scenario for a five-phase system, as the CMV waveform contains all possible CMV levels. This results in $\Delta_p = 1$, $\Delta_s = 1/5$, $N_L = 6$ and $N_T = 10$.

In the following, some of the most prominent modulation techniques, which reduce these CMV related figures-of-merit are reviewed.

4.2. Discontinuous PWM techniques

Regarding multiphase systems, the discontinuous DPWM-MAX, DPWM-MIN, DPWM-V1, and DPWM-V2 three-phase variants have been adapted for a five-phase inverter in [68], and their performance is compared with the previously explained 2L-SV-PWM, 2L2M-SV-PWM and 4L-SV-PWM techniques.

Fig. 12(a) illustrates the vector representation and CMV waveform obtained by using one of the techniques implemented in [68], namely 4L-D-PWM, which synthesizes the reference output voltage vector \mathbf{V}_{ref} by using four large active vectors. In this particular case, the LR remains the same as for 4L-SV-PWM, since \mathbf{V}_{ref} is synthesized with the same vectors. Thus, the maximum magnitude of \mathbf{V}_{ref} is of $0.5257 V_{DC}$ and $M_a \in [0, 1.051]$ (Fig. 11(b)). Unlike 4L-SV-PWM, CMV figures-of-merit are reduced to $\Delta_p = 3/5$, $N_L = 3$ and $N_T = 8$ (see Fig. 12(b)), however, there are different Δ_s values, $1/5$ and $2/5$.

In general, such discontinuous modulation techniques reduce the CMV by not applying both zero vectors during a modulation period T_{sw} and by not switching one of the inverter's legs. This eliminates one of the CMV levels, which is beneficial. However, because the zero vectors cause the highest CMV levels ($\pm V_{DC}/2$), avoiding them is critical for an effective reduction of the CMV. Thus, the most relevant RCMV-PWM

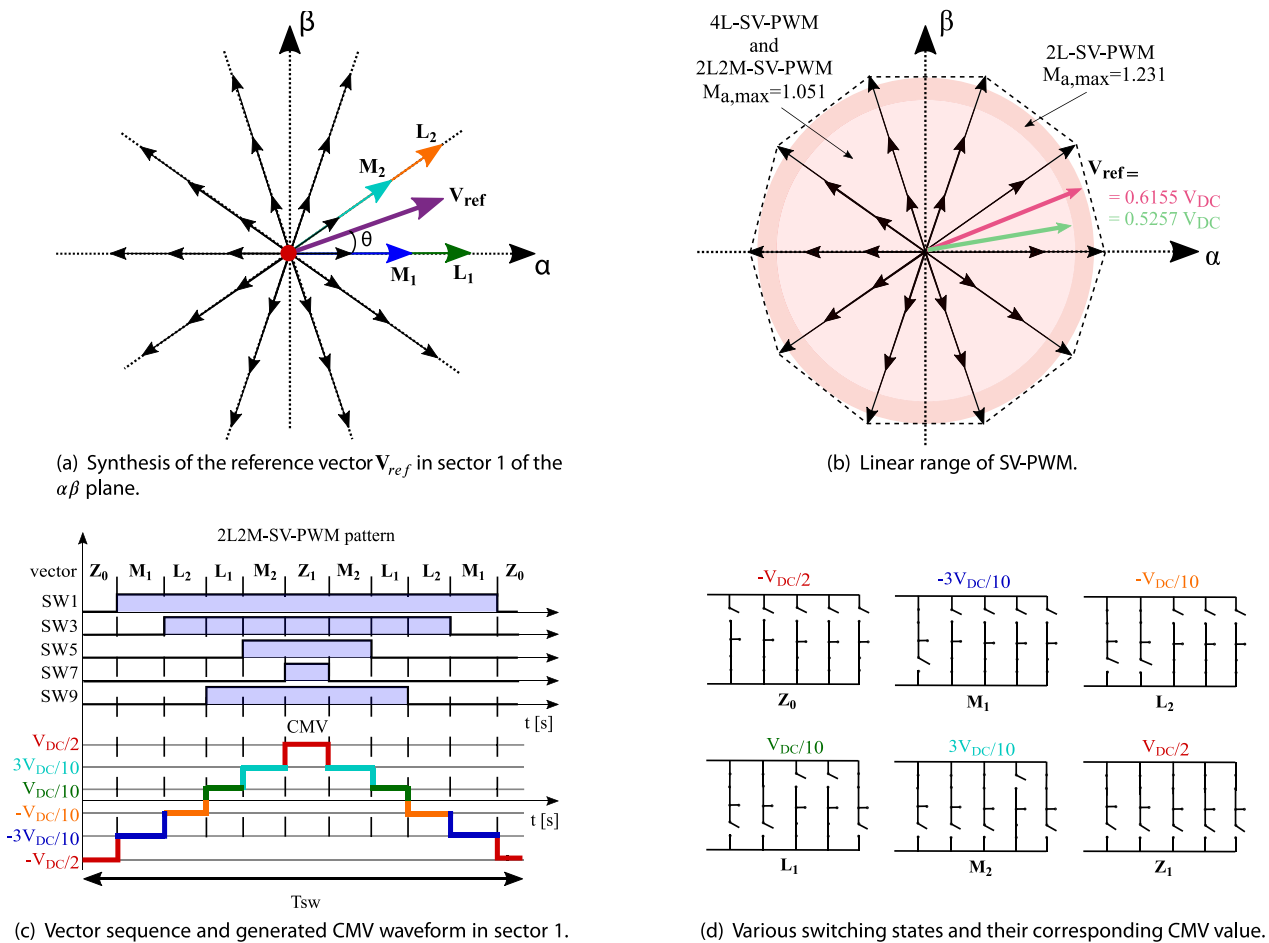


Fig. 11. Vector representation of the 2L2M-SV-PWM technique for five-phase converters along with the switching states and associated CMV levels.

algorithms for five-phase inverters, which completely avoid using zero vectors, are described and compared below.

4.3. Reduced-CMV PWM (RCMV-PWM) techniques

(A) *active zero-state PWM (AZS-PWM)*. The well-known three-phase AZS-PWM technique can be extended for star-connected m -phase systems, in general, and for five-phase systems, in particular. As well as the SV-PWM technique, AZS-PWM can be implemented in different ways, depending on the particular selection of the available active vectors:

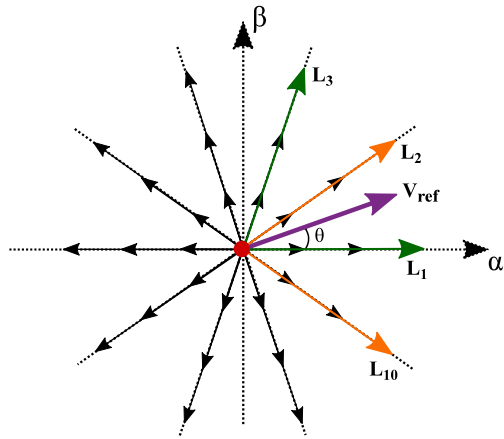
- The 2L2M-AZS-PWM variant makes use of two medium and two large vectors to synthesize V_{ref} , in addition to two active vectors, with the same modulus and opposite phase, to avoid the application of zero vectors (Fig. 13(a)) [86]. As a result, the maximum achievable output voltage is $0.5257 V_{DC}$, where $M_a \in [0, 1.051]$ (same as in 2L2M-SV-PWM, Fig. 11(b)). Regarding the CMV, 2L2M-AZS-PWM obtains better figures-of-merit when compared to the 2L2M-SV-PWM technique, i.e., $\Delta_p = 3/5$, $\Delta_s = 1/5$, $N_L = 4$ and $N_T = 6$ are obtained (Fig. 13(b)), since zero vectors are avoided.
- The 4L-AZS-PWM variant has also been developed in [86]. This variant only makes use of large vectors to synthesize V_{ref} (Fig. 14(a)). Thus, the LR of this technique is the same as the previous one (see Fig. 11(b)). It could also be possible to apply small vectors to fill the application time of zero vectors, as they produce the same CMV levels. However, the utilization of large vectors is recommended, since they produce lower harmonics in the xy -plane [86]. Likewise, since medium and zero vectors are

avoided, the only two CMV levels to be synthesized are $\pm V_{DC}/10$ (Fig. 14(b)), this resulting in $\Delta_p = \Delta_s = 1/5$, $N_L = 2$ and $N_T = 10$.

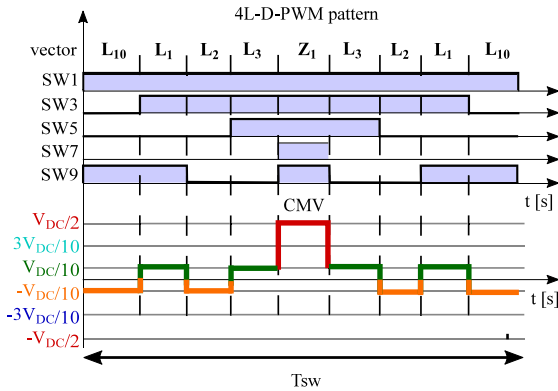
(B) *remote-state PWM (RS-PWM)*. Similar to three-phase power inverters, all odd or even vectors produce the same CMV value, regardless their type (small, medium or large). Thus, the RS-PWM concept used for three-phase system can be adapted to the multiphase scenario. For example, [122] proposes to use only the five medium odd or even vectors to generate V_{ref} (Fig. 15(a)). This technique, here named 5M-RS-PWM, completely eliminates CMV transitions (Fig. 15(c)). CMV equals $-3V_{DC}/10$ when using odd vectors, and $+3V_{DC}/10$ for even vectors. Its associated CMV figures-of-merit are $\Delta_p = \Delta_s = N_T = 0$ and $N_L = 1$. However, this solution has an important drawback, as the LR is greatly reduced ($M_a \in [0, 0.646]$), thus resulting in a maximum output voltage of $0.323 V_{DC}$; see Fig. 15(b). This LR could be insufficient for a great number of drive applications that must operate both close to the base speed and in field weakening.

In order to extend the LR of the previous technique, an obvious solution is to use only odd or even large active vectors [122], leading to the 5L-RS-PWM variant (Fig. 16(a)). By doing so, the LR is increased up to $0.523 V_{DC}$ and ($M_a \in [0, 1.046]$; Fig. 16(b)). Again, CMV variations are completely eliminated and obtaining a CMV value of $\pm V_{DC}/10$ (Fig. 16(c)). Thus, the CMV figures-of-merit of this modulation variant equal the ones of 5M-RS-PWM technique. However, the absolute value of the CMV is lower when large vectors are used.

Although both variants completely suppress CMV variations, they have various disadvantages when compared to the AZS-PWM techniques previously reviewed. Apart from the reduced LR, which is an important limiting factor depending on the application, switching losses



(a) Synthesis of the reference vector V_{ref} in sector 1.



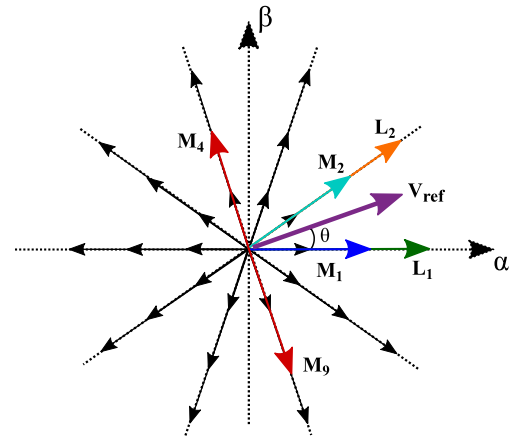
(b) Vector sequence and generated CMV waveform in sector 1.

Fig. 12. Vector representation of the 4L-D-PWM technique along with the switching states and associated CMV levels.

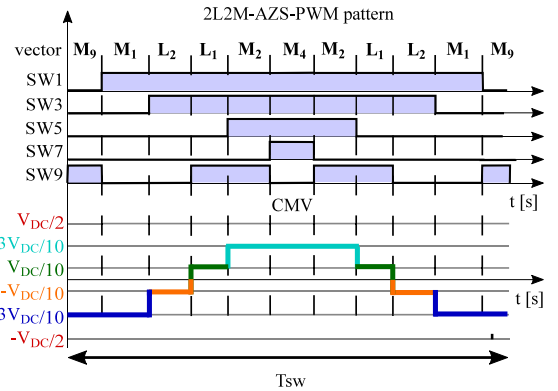
are increased, as a higher number of commutations is required for each modulation period T_{sw} . Additionally, harmonic distortion of current (THD_i) is also increased, due to the reduction of the available vectors.

(C) *near-state PWM (NS-PWM)*. The well-known three-phase NS-PWM technique can be also adapted to the multiphase scenario [123]. As in the three-phase version, sectors must be shifted to obtain the new sector distribution, particularly 18° for a five-phase system (Fig. 17(a)). This technique, named here as 5L-NS-PWM, requires the utilization of five active vectors each T_{sw} for the synthesis of V_{ref} . Specifically, the nearest active vector to the reference one and four adjacent vectors (two in the left side and two in the right side of V_{ref}) are used (Fig. 17(a)).

By using five large vectors, the linear range is considerably reduced. Not only the maximum output voltage ($M_a \in [0.8820, 1.0515]$ and $V_{ref,max} = 0.5257 V_{DC}$) but also the minimum voltage vector is limited ($V_{ref,min} = 0.441 V_{DC}$); see Fig. 17(b). This is a significant drawback for applications where the drive must be torque or speed regulated from standstill, as in traction applications. Thus, this technique should be hybridized with other modulation techniques until V_{ref} lies within the aforementioned LR. Regarding CMV, the CMV waveform is quite similar to the one obtained with 4L-AZS-PWM, since the produced CMV voltage levels are the same ($\pm V_{DC}/10$; $\Delta_p = \Delta_s = 1$ and $N_L = 2$). However, this technique has a superior performance with respect to the N_T , as this figure-of-merit reduces from 10 to 8 (Fig. 17(c)).



(a) Synthesis of the reference vector V_{ref} in sector 1.



(b) Vector sequence and generated CMV waveform in sector 1.

Fig. 13. Vector representation of the 2L2M-AZS-PWM technique along with the switching states and associated CMV levels.

4.4. Other modulation and control techniques for CMV reduction

In addition to all these modulation techniques, other SV-based approaches have been proposed to reduce the CMV in five-phase systems.¹⁶ For example, the hybrid technique presented in [60] combines the AZS-PWM and RS-PWM solutions. In particular, four medium and two large vectors (all even or odd) are used to synthesize V_{ref} (Fig. 18(a)), maintaining the LR of 5L-RS-PWM as $0.523 V_{DC}$ and $M_a \in [0, 1.046]$ (Fig. 18(b)). This allows improving CMV figures-of-merit to $\Delta_p = 2/5$, $\Delta_s = 2/5$, $N_L = 2$ and $N_T = 2$ (Fig. 18(c)), but increasing the number of switchings of the converter devices, and consequently, the switching losses.

Apart from all of that, [140] proposes to use only odd or even vectors but including a zero vector to synthesize V_{ref} . However, this technique has worse characteristics than the previous one and, therefore, it is not represented in this work. Nevertheless, this latter approach has already been considered for modulation techniques of three-phase converters, such as the CCMV-PWM [25,28].

¹⁶ Similarly, CB-PWM techniques could be also considered. There is no clear agreement as to which modulation approach is better. Based on the most of two-level modulation studies, it seems a general belief that the CB method is more efficient and flexible, whereas SV yields better harmonics performance and can handle more conveniently overall switching patterns and constraints [138]. However, the complexity increases as the number of phases do. Therefore, CB seems to be a better alternative for CMV elimination in topologies with high number of phases. For this reason, some works [87,139] propose CB modulation techniques to reduce the CMV.

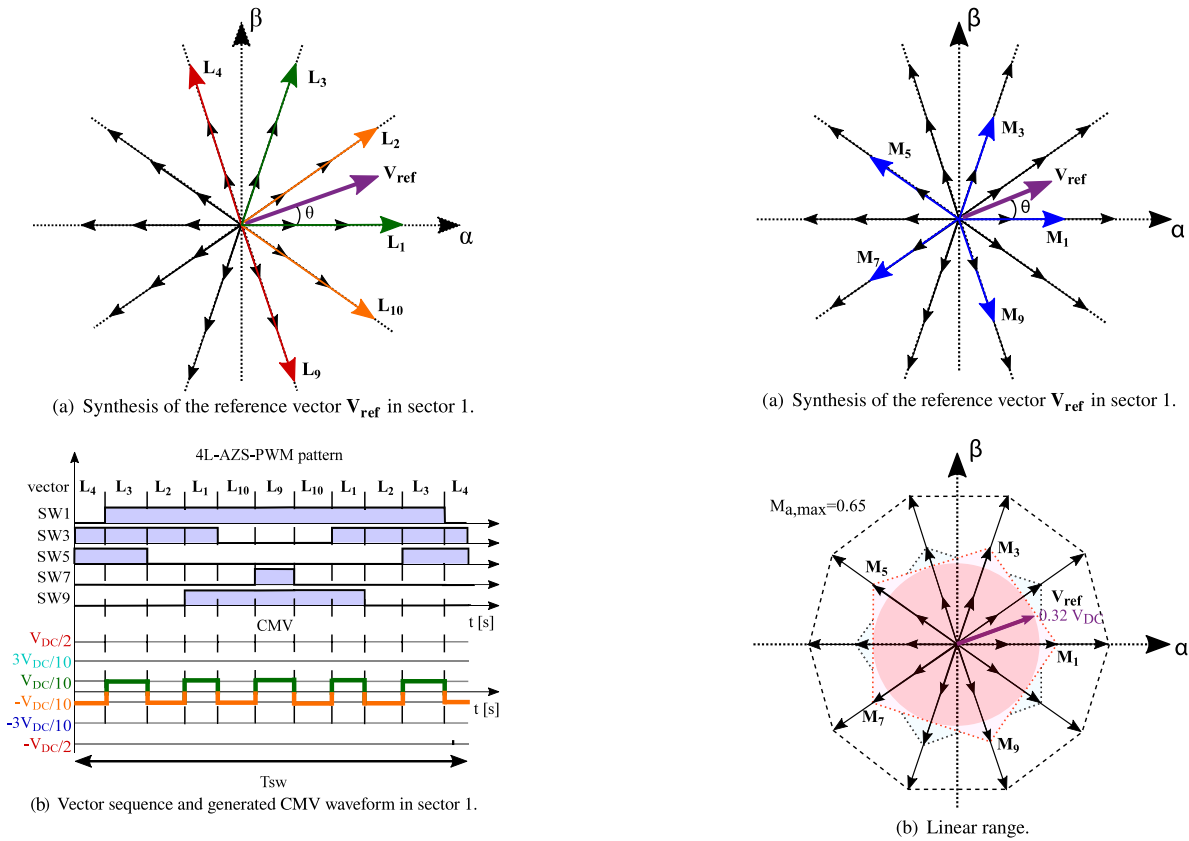


Fig. 14. Vector representation of the 4L-AZS-PWM technique along with the switching states and associated CMV levels.

Finally, it should be noted that all the previous techniques would be included within the PWM-based techniques and they can be implemented in an open- and closed-loop. Nevertheless, there are other techniques such as those based on the model predictive control (MPC; Fig. 19(b)), which are characterized by eliminating conventional modulation and working in a closed-loop in order to control several variables of the system. This control is valid throughout the linear range and even in the overmodulation range [132]. Particularly, the control technique known as model predictive current control (MPCC) is being extensively used in multiphase VSIs and drive systems [122,141–144]. This last technique is aimed at predicting the output current for all possible vectors and selecting the optimal voltage vector using a predefined cost function (Fig. 19(a)). To do this, two approaches can be followed, either using cost function optimization-based methods, or voltage vector preselection-based methods (Fig. 19(b)).

In the first case, since different control variables can be included in the cost function, different MPCC methods in converters can include the CMV variable and penalize the vectors that generate higher CMV [146]. In this sense, in [147] a comprehensive analysis of the CMV reduction using MPC in a five-phase drive has been realized. The proposal uses two different weighting factors to penalize long and medium vectors. Different adjustments of the weights in the cost function are analysed to find a good balance between low current distortion and CMV reduction. This proposal achieves a reduction of the peaks of the CMV up to 80 % at the cost of increasing the THD_i of the stator and depending on the vector penalty. However, although this last method can reduce the CMV, its main drawback is the difficulty of properly tuning the weights in the cost function [148].

The second type of method to reduce the CMV would be the one that does not include the CMV term in its cost function and, thus, eliminates the empirical parameters tuning. In this way, the modulation technique

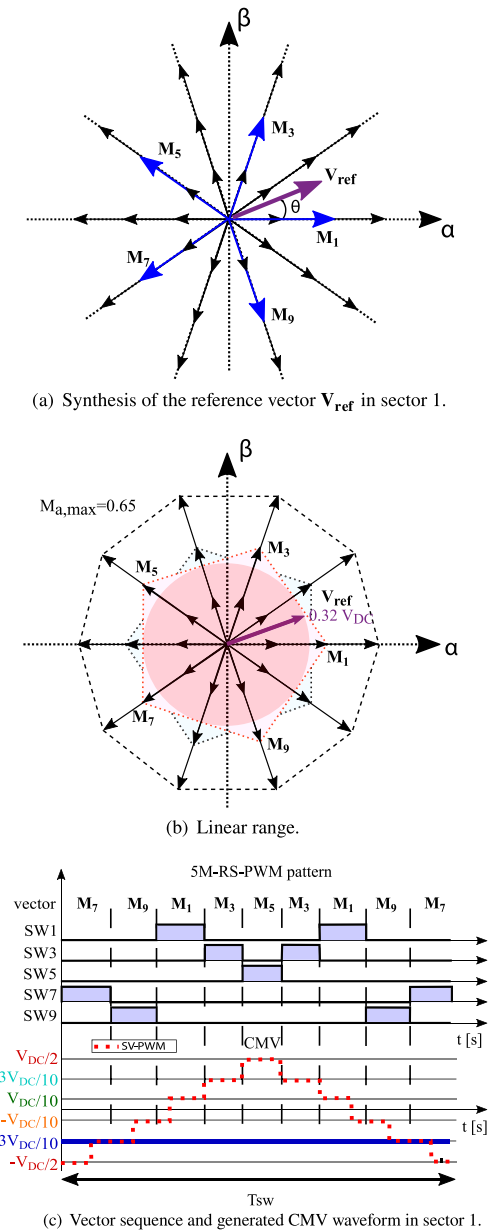
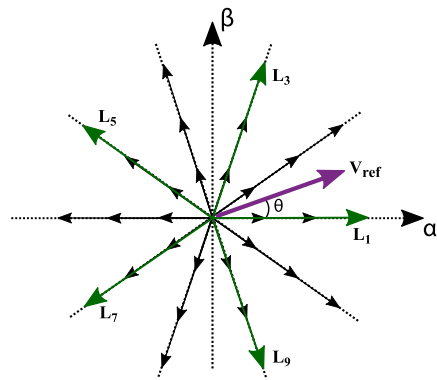


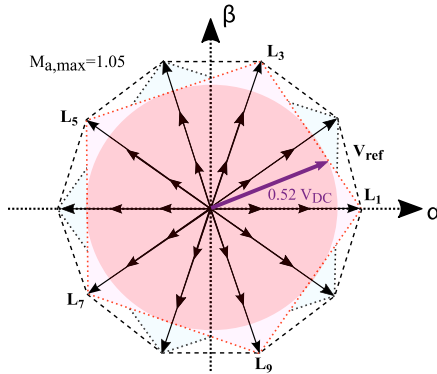
Fig. 15. Vector representation of the 5M-RS-PWM technique along with the switching states and associated common-mode voltage levels.

is only based on the preselection of voltage vectors. There are different methods based on this approach in the context of multiphase inverters, which are also called finite set predictive control methods [122,149, 150]. For example, in [149], an improved predictive model of current control (IMPCC) is implemented in conjunction with the use of virtual voltage vectors. The technique, called IMPCC1 or IMPCC2 depending on whether it uses an asymmetrical or a symmetrical switching pattern respectively, also manages to reduce the CMV ($\Delta_p = 1/5$, $\Delta_S = 1/5$, $N_L = 2$ and $N_T = 5$ for IMPCC1, and $\Delta_p = 1/5$, $\Delta_S = 1/5$, $N_L = 2$ and $N_T = 10$ for IMPCC2). Likewise, in [150] two new definitions are proposed to construct virtual voltage vectors. The first, called MPCC- V^3 -RCMV1, reduces the CMV to $\Delta_p = 0$, $\Delta_S = 0$, $N_L = 1$ and $N_T = 0$. The second, called MPCC- V^3 -RCMV2, reduces the CMV to $\Delta_p = 1/5$, $\Delta_S = 1/5$, $N_L = 2$ and $N_T = 4$.

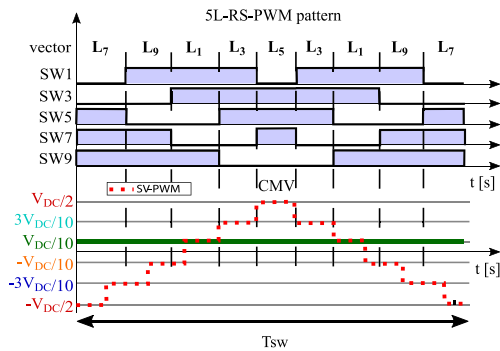
It can be concluded that any preselection of voltage vectors can be used in any MPCC technique or finite set predictive control technique. In fact, in [122] it is proposed to use 5M-RS-PWM as the sequence



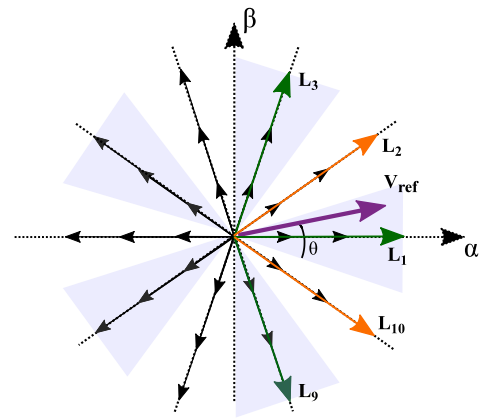
(a) Synthesis of the reference vector V_{ref} in sector 1.



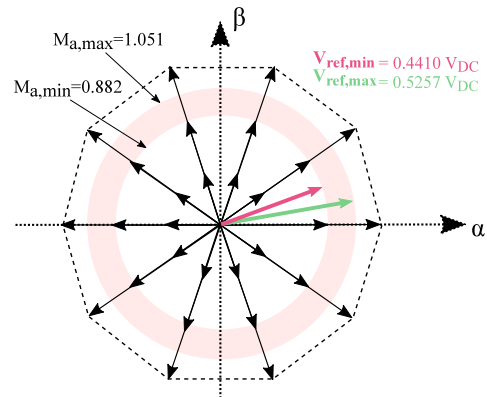
(b) Linear range.



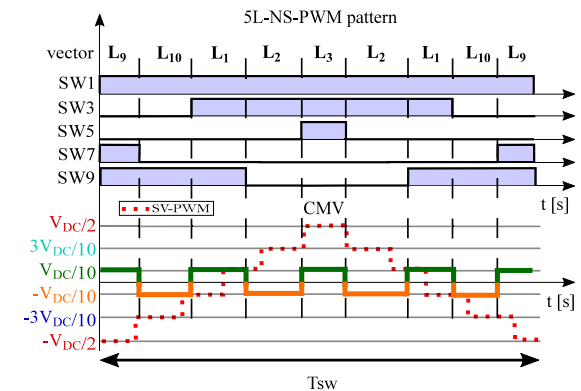
(c) Vector sequence and generated CMV waveform in sector 1.



(a) Synthesis of the reference vector V_{ref} in sector 1.



(b) Linear range.



(c) Vector sequence and generated CMV waveform in sector 1.

Fig. 16. Vector representation of the 5L-RS-PWM technique along with the switching states and associated common-mode voltage levels.

Fig. 17. Vector representation of the 5L-NS-PWM technique along with the switching states and associated common-mode voltage levels.

of vectors to be applied in the finite set predictive control technique. Therefore, any modulation technique of those reviewed in the previous sections could be proposed together with an MPC. In this sense, as a summary, Table 9 presents the CMV figures-of-merit, CMV waveforms, the linear range, and some references of all modulation techniques for CMV mitigation of star-connected five-phase systems reviewed in this work.¹⁷

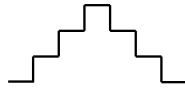

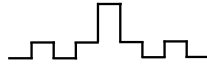
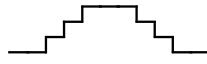

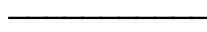
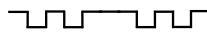

¹⁷ Additionally, it is worth noting that in addition to these PWM algorithms, generalized reduced CMV modulation techniques for a different number of voltage levels and phases have been proposed in [151,152]. However, modulations for converters with more than two levels lie out of the scope of this work.

5. Conclusions

From this comprehensive review, it can be confirmed that CMV in electric drives has become a popular topic due to the problems associated with this voltage. The existence of several stray common-mode impedance paths between the inverter and the motor frame allows leakage currents to flow through the motor at every CMV variation. These currents lead to motor bearing failures, in addition to other CMV-derived problems such as EMI or deterioration of the motor stator insulation. It is expected that such problems will be even more serious in the near future with the widespread introduction of wide-bandgap devices.

Table 9

CMV waveforms and figures-of-merit of the reviewed modulation techniques for CMV mitigation used in five-phase star-connected converters (conventional SV-PWM is incorporated for reference).

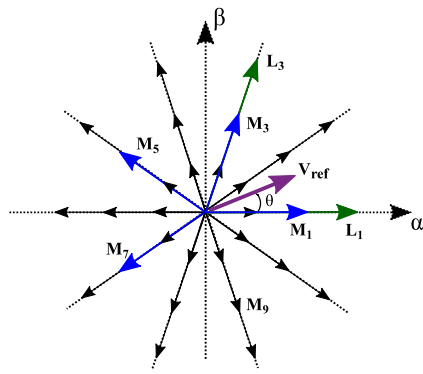
Modulation technique	Figures-of-merit				Increase/decrease (%) over conventional SV-PWM				CMV waveform	Linear range	Refs.
	Δ_p	Δ_s	N_L	N_T	Δ_p	Δ_s	N_L	N_T			
Conventional two-level three-phase voltage source inverter											
Conventional SV-PWM	1	1/3	4	6	-	-	-	-		$0 \leq M_a \leq 1.15$	[28,74]
Two-level five-phase inverters with star-connected load											
2L2M-SV-PWM	1	1/5	6	10	0	-40	50	66.7		$0 \leq M_a \leq 1.05$	[134,136]
4L-D-PWM	3/5	2/5	3	8	-40	20	-25	33.3		$0 \leq M_a \leq 1.05$	[68]
2L2M-AZS-PWM	3/5	1/5	4	6	-40	-40	0	0		$0 \leq M_a \leq 1.05$	[86]
4L-AZS-PWM	1/5	1/5	2	10	-80	-40	-50	66.7		$0 \leq M_a \leq 1.05$	[86]
5L-RS-PWM	0	0	1	0	-100	-100	-75	-100		$0 \leq M_a \leq 1.04$	[122]
5L-NS-PWM	1/5	1/5	2	8	-80	-40	-50	33.3		$0.88 \leq M_a \leq 1.05$	[123]
2L4M-Hyb.-PWM	2/5	2/5	2	2	-60	20	-50	-66.7		$0 \leq M_a \leq 1.05$	[60]
MPC with cost function optimization	* It depends on how each vector is penalized and what CMV value generates each vector.								-	-	[147]
MPC with voltage vector preselection	* It depends on the voltage vector preselection used. Any of the above techniques could be applied, in addition to others.								-	-	[122,149,150]

The key role of multiphase inverters in modern electric drives and their relation to CMV has been discussed in this paper. From this review, the following relevant conclusions have been obtained:

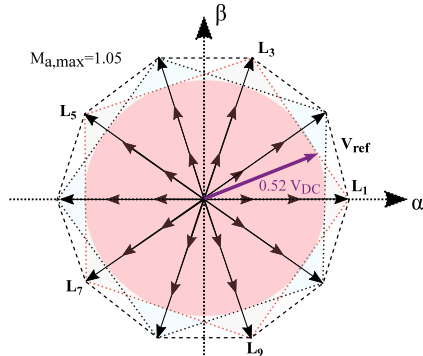
1. Multiphase technologies provide a number of well-known advantages over conventional three-phase systems such as power splitting, improved efficiency, lower torque and DC-link current ripple, additional degrees of freedom and fault tolerance. Such degrees of freedom can be effectively used for CMV mitigation.
2. The most common architectures are the multiphase inverters feeding a star-connected load, the $(m + 1)$ -leg converters, the multiple three-phase configurations and the open-end multiphase converters. In particular, star-connected five-phase and dual three-phase systems are the most popular ones in both industry and academia thanks to their trade-off between features and complexity.
3. By analysing various possible CMV waveform patterns, it can be concluded that, in many cases, it is not possible to assess the superiority of one pattern over the others. If by applying a given pattern reliability improvement is targeted, EMI can be penalized, and vice versa. Field engineers are responsible for

selecting the most appropriate solution depending on the specific requirements of the application. For this purpose, a number of figures-of-merit have been defined to provide a clear picture of the CMV issue for each case.

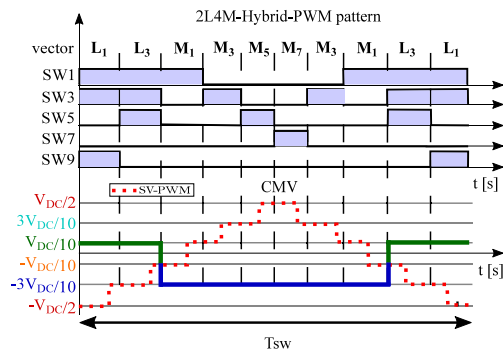
4. Regarding phase- or leg-count, without applying a specific modulation technique, the analysis carried out shows that Δ_s figure-of-merit decreases as the phase-number increases, while N_L and N_T increase and Δ_p remains constant. Thus, the multiphase hardware solution must be complemented with an appropriate modulation technique to take full advantage of its CMV mitigation potential.
5. Regarding modulation algorithms, when these techniques are used to reduce the CMV, other parameters such as efficiency and/or harmonic distortion are usually affected, regardless of whether the technique has been implemented following the CB or SV approach. Therefore, the most suitable modulation technique will depend on the requirements of each application. Based on this review, it has been concluded that the most promising multiphase modulation techniques when it comes to reducing CMV are those of the RCMV-PWM family. When the main objective is to reduce the CMV, the 5L-RS-PWM technique



(a) Synthesis of the reference vector V_{ref} in sector 1.



(b) Linear range.

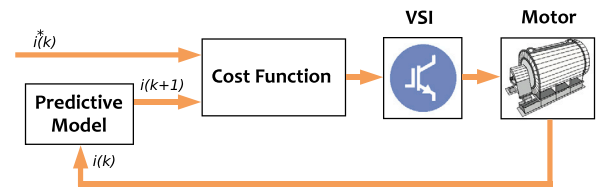


(c) Vector sequence and generated CMV waveform in sector 1.

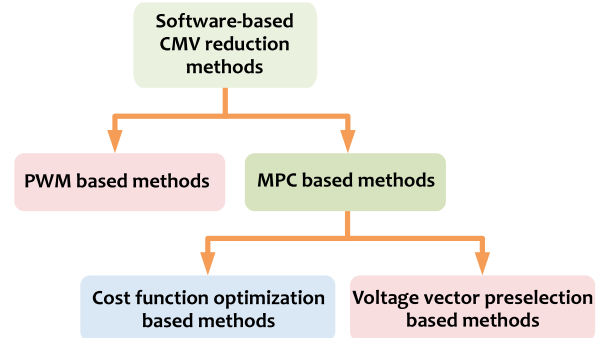
Fig. 18. Vector representation of the 2L4M-Hybrid-PWM technique along with the switching states and associated common-mode voltage levels.

can be highlighted for star-connected five-phase systems, as it completely eliminates CMV variations while maintaining a wide linear range. Likewise, the 5L-NS-PWM technique allows to greatly reduce the CMV when compared to 2L2M-SV-PWM. In addition, since this PWM algorithm reduces the number of commutations by 20 %, it also reduces the inverter losses. However, when reducing CMV, other aspects such as low order output voltage harmonics or the maximum utilization of the DC bus voltage must always be considered. In this sense, the linear range of 5L-NS-PWM could be insufficient for a great number of electric drive applications such as for hybrid or electric vehicles.

Finally, it can be stated that the next research steps on CMV mitigation in multiphase systems should be focused on high power applications, where inverters with a high phase-number (more than nine) will be usually considered. Existing RCMV-PWM techniques can be extended to those converters or, taking advantage of the additional



(a) General block diagram of an MPCC for a VSI drive [123].



(b) Classification of software-based CMV reduction methods [145].

Fig. 19. Inclusion of predictive models and cost functions in modulation techniques for CMV reduction [122,145].

degrees of freedom, new RCMV-PWM algorithms can be developed. In addition, since some RCMV-PWM modulation techniques have a reduced linear range, their hybridization with other modulation techniques must be considered to achieve a CMV reduction in a wider linear range. This aspect is specially relevant in electromobility applications, such as in electric vehicles. Likewise, since fault-tolerance is one of the most attractive features in multiphase drive systems, multi-objective PWM schemes can be proposed to reduce the CMV under different fault scenarios. Thus, it is confirmed that there is still a wide variety of research topics on CMV mitigation of multiphase systems.

Declaration of competing interest

The authors declare that they have no known competing financial interests or personal relationships that could have appeared to influence the work reported in this paper.

Acknowledgements

This work has been supported in part by the Government of the Basque Country within the fund for research groups of the Basque University system IT978-16 and the research program ELKARTEK (project ENSOL2-KK-2020/00077). In addition, this work has been supported by the Secretaria d'Universitats i Recerca del Departament d'Empresa i Coneixement de la Generalitat de Catalunya, Spain, as well as the Ministerio de Ciencia, Innovacion y Universidades of Spain within the projects PID2019-111420RB-I00, PID2020-115126RB-I00 and FEDER funds, Spain.

References

- [1] Ray AL, Couse D. Cement plant fan efficiency upgrades. *IEEE Trans Ind Appl* 2017;53(2):1562–8.
- [2] Oliveira F, Ukil A. Comparative performance analysis of induction and synchronous reluctance motors in chiller systems for energy efficient buildings. *IEEE Trans Ind Inform* 2019;15(8):4384–93.
- [3] Khan KR, Miah MS. Fault-tolerant BLDC motor-driven pump for fluids with unknown specific gravity: an experimental approach. *IEEE Access* 2020;8:30160–73.

- [4] Shukla S, Singh B. Reduced current sensor based solar PV fed motion sensorless induction motor drive for water pumping. *IEEE Trans Ind Inform* 2019;15(7):3973–86.
- [5] Besselmann TJ, Cortinovis A, Van de moortel S, Ditlefsen A, Mercanzog M, Fretheim H, Jorg P, Lunde E, Knutsen T, Stava TO. Increasing the robustness of large electric driven compressor systems during voltage dips. *IEEE Trans Ind Appl* 2018;54(2):1460–8.
- [6] van Werkhoven M, Werle R, Brunner CU. Policy guidelines for motor driven units. Part 1: Analysis of standards and regulations for pumps, fans and compressors. Technical report, Electric Motor Systems EMSA; 2016.
- [7] Wiechmann EP, Aqueveque P, Burgos R, Rodriguez J. On the efficiency of voltage source and current source inverters for high-power drives. *IEEE Trans Ind Electron* 2008;55(4):1771–82.
- [8] McKerracher C, Izadi-Najafabadi A, Donovan AO, Albanese N, Soulopoulos N, Doherty D, Boers M, Fisher R, Cantor C, Frith J, Mi S, Grant A. Electric vehicle outlook - bloomberg's forecast for annual electric vehicle sales. Technical report, Bloomberg; 2020, URL: <https://about.bnef.com/electric-vehicle-outlook/>.
- [9] Orłowska-Kowalska T, Dybkowski M. Industrial drive systems. Current state and development trends. *Power Electron Drives* 2016;1(1):5–25.
- [10] Delaney DE, Beloit R. GMEE “global motor energy efficiency” program update. In *Proc. of the international conference on energy efficiency in motor driven systems (eemods)*, 2017, pp. 285–92.
- [11] Leon JI, Vazquez S, Franquelo LG. Multilevel converters: control and modulation techniques for their operation and industrial applications. *Proc IEEE* 2017;105(11):2066–81.
- [12] Fong J, Ferreira F, Silva A, de Almeida A. IEC61800-9 system standards as a tool to boost the efficiency of electric motor driven systems worldwide. *Inventions* 2020;5(20):1–15.
- [13] Lee J, Jung D, Lim J, Lee K, Lee J. A study on the synchronous reluctance motor design for high torque by using RSM. *IEEE Trans Magn* 2018;54(3):1–5.
- [14] Manual for industrial motor systems assessment and optimization. Technical report, United Nations Industrial Development Organization (UNIDO); 2018.
- [15] IEC 61800-9-2. Ecodesign for power drive systems, motor starters, power electronics and their driven applications - energy efficiency indicators for power drives systems and motor starters. Technical report, International Electrotechnical Commission (IEC); 2017.
- [16] de Almeida A, Falkner H, Fong J, Jugdoyal K. Eup lot 30: electric motors and drives. task 2: economic and market analysis ener/c3/413-2010. Technical report, ISR - University of Coimbra; 2014.
- [17] Advanced Manufacturing Office. A sourcebook for industry - improving motor and drive system performance. Technical report, U.S. Department of Energy - Energy Efficiency and Renewable energy; 2014.
- [18] Scelba G, Donato GD, Scarcella G, Capponi FG, Cacciato M, Caricchi F. On the reliability of electrical drives for safety-critical applications. In *Proc. of the international conference on energy efficiency in motor driven systems (eemods)*, 2017, pp. 313–27.
- [19] Wu B, Pontt J, Rodriguez J, Bernet S, Kouro S. Current-source converter and cycloconverter topologies for industrial medium-voltage drives. *IEEE Trans Ind Electron* 2008;55(7):2786–97.
- [20] Migliazza G, Buticchi G, Carfagna E, Lorenzani E, Madonna V, Giangrande P, Galea M. DC Current control for a single-stage current source inverter in motor drive application. *IEEE Trans Power Electron* 2021;36(3):3367–76.
- [21] Andrews J, Gheeth AH, Ganesan V. Practical guidelines for planning network connection of electric drive systems. In *Proc. of the petroleum and chemical industry conference europe (pic europe)*, 2017, pp. 1–11.
- [22] Steczek M, Chudzik P, Lewandowski M, Szelg A. PSO-Based optimization of DC-link current harmonics in traction VSI for an electric vehicle. *IEEE Trans Ind Electron* 2020;67(10):8197–208.
- [23] Sridharan S, Krein PT. Minimization of system-level losses in VSI-based induction motor drives: offline strategies. *IEEE Trans Ind Appl* 2017;53(2):1096–105.
- [24] Asefi M, Nazarzadeh J. Survey on high-frequency models of PWM electric drives for shaft voltage and bearing current analysis. *IET Electr Syst Transp* 2017;7(3):179–89.
- [25] Concari L, Barater D, Toscani A, Concari C, Franceschini G, Buticchi G, Liserre M, Zhang H. Assessment of efficiency and reliability of wide band-gap based H8 inverter in electric vehicle applications. *Energies* 2019;12(1922):1–17.
- [26] Ali S, Vijaya Kumar Reddy V, Surya Kalavathi M. Performance of space vector PWM based induction motor drive using dspace. *Int J Innov Technol Explor Eng* 2019;8(4S2):400–4.
- [27] Tan B, Gu Z, Shen K, Ding X. Third harmonic injection SPWM method based on alternating carrier polarity to suppress the common mode voltage. *IEEE Access* 2019;7:9805–16.
- [28] Robles E, Fernandez M, Ibarra E, Andreu J, Kortabarria I. Mitigation of common mode voltage issues in electric vehicle drive systems by means of an alternative AC-decoupling power converter topology. *Energies* 2019;12:3349.
- [29] Huang J, Li K. Suppression of common-mode voltage spectral peaks by using rotation reverse carriers in sinusoidal pulse width modulation three-phase inverters with CFM. *IET Power Electron* 2020;13(6):1246–56.
- [30] Robles E, Fernandez M, Andreu J, Ibarra E, Ugalde U. Advanced power inverter topologies and modulation techniques for common-mode voltage elimination in electric motor drive systems. *Renew Sustain Energy Rev* 2021.
- [31] Choudhury A, Pillay P, Williamson SS. Modified DC-bus voltage balancing algorithm for a three-level neutral-point-clamped PMSM inverter drive with reduced common-mode voltage. *IEEE Trans Ind Appl* 2016;52(1):278–92.
- [32] Zhang X, Wu X, Geng C, Ping X, Chen S, Zhang H. An improved simplified PWM for three-level neutral point clamped inverter based on two-level common-mode voltage reduction PWM. *IEEE Trans Power Electron* 2020;35(10):11143–54.
- [33] Jiang W, Wang P, Ma M, Wang J, Li J, Li L, Chen K. A novel virtual space vector modulation with reduced common-mode voltage and eliminated neutral point voltage oscillation for neutral point clamped three-level inverter. *IEEE Trans Ind Electron* 2020;67(2):884–94.
- [34] Guo X, Wei B, Zhu T, Lu Z, Tan L, Sun X, Zhang C. Leakage current suppression of three-phase flying capacitor PV inverter with new carrier modulation and logic function. *IEEE Trans Power Electron* 2018;33(3):2127–35.
- [35] Arasteh M, Rahmati A, Farhangi S, Abrishamifar A. Common mode voltage reduction in a flying capacitor inverter. In *Proc. of the power electronic, drive systems and technologies conference (pedstc)*, 2010, p. 212–7.
- [36] Mendes MAS, Peixoto ZMA, Seixas PF, Donoso-Garcia P. A space vector PWM method for three-level flying-capacitor inverters. In *Proc. of the IEEE annual power electronics specialists conference (pesc)*, Vol. 1, 2001, p. 182–7.
- [37] da Silva MM, Pinheiro H. Voltage balancing in flying capacitor converter multilevel using space vector modulation. In *Proc. of the international symposium on power electronics for distributed generation systems (pedg)*, 2017, p. 1–5.
- [38] Leon JI, Kouro S, Vazquez S, Portillo R, Franquelo LG, Carrasco JM, Rodriguez J. Multidimensional modulation technique for cascaded multilevel converters. *IEEE Trans Ind Electron* 2011;58(2):412–20.
- [39] Loh PC, Holmes DG, Fukuta Y, Lipo TA. Reduced common-mode modulation strategies for cascaded multilevel inverters. *IEEE Trans Ind Appl* 2003;39(5):1386–95.
- [40] Nguyen TT, Nguyen N, Prasad NR. Eliminated common-mode voltage pulsewidth modulation to reduce output current ripple for multilevel inverters. *IEEE Trans Power Electron* 2016;31(8):5952–66.
- [41] Gupta AK, Khambadkone AM. A space vector modulation scheme to reduce common mode voltage for cascaded multilevel inverters. *IEEE Trans Power Electron* 2007;22(5):1672–81.
- [42] Sonti V, Dhara S, Kukade P, Jain S, Agarwal V. Analysis for the minimization of leakage and common mode currents in cascaded Half-Bridge PV fed multilevel inverter. *IEEE J Emerg Sel Top Power Electron* 2019;7(4):2443–52.
- [43] Kontos EM, Tsolaridis G, Teodorescu R, Bauer P. Full-bridge MMC DC fault ride-through and STATCOM operation in multi-terminal HVDC grids. *Bull Polish Acad Sci: Tech Sci* 2017;65:653–62.
- [44] Du S, Wu B, Zargari N. Common-mode voltage minimization for grid-tied modular multilevel converter. *IEEE Trans Ind Electron* 2019;66(10):7480–7.
- [45] Du S, Dekka A, Wu B, Zargari N. Modular multilevel converters: analysis, control, and applications - part iii: applications of modular multilevel converters. 2017.
- [46] Poorfakhraei A, Narimani M, Emadi A. A review of multilevel inverter topologies in electric vehicles: Current status and future trends. *IEEE Open J Power Electron* 2021;2:155–70.
- [47] Choudhury A, Pillay P, Williamson SS. Comparative analysis between two-level and three-level DC/AC electric vehicle traction inverters using a novel DC-link voltage balancing algorithm. *IEEE J Emerg Sel Top Power Electron* 2014;2(3):529–40.
- [48] Barrero F, Duran M. Recent advances in the design, modeling, and control of multiphase machines - Part I. *IEEE Trans Ind Electron* 2016;63(1):449–58.
- [49] Duran M, Barrero F. Recent advances in the design, modeling, and control of multiphase machines - Part II. *IEEE Trans Ind Electron* 2016;63(1):459–68.
- [50] Karttunen J, Kallio S, Peltoniemi P, Silventoinen P, Phyrnonen O. Decoupled vector control scheme for dual three-phase permanent magnet synchronous machines. *IEEE Trans Ind Electron* 2014;61(5):2185–96.
- [51] Liu Z, Zheng Z, Xu L, Wang K, Li Y. Current balance control for symmetrical multiphase inverters. *IEEE Trans Power Electron* 2016;31(6):4005–12.
- [52] Deng Q, Wang Z, Chen C, Czarkowski D, Kazmierczuk MK, Zhou H, Hu W. Modeling and control of inductive power transfer system supplied by multiphase phase-controlled inverter. *IEEE Trans Power Electron* 2019;34(9):9303–15.
- [53] Belkhou S, Jain S. Optimized switching PWM technique with common-mode current minimization for five-phase open-end winding induction motor drives. *IEEE Trans Power Electron* 2019;34(9):8971–80.
- [54] Parsa L, Toliyat H. Five-phase permanent-magnet motor drives. *IEEE Trans Ind Appl* 2005;1(4):30–7.
- [55] Zheng P, Wu F, Lei Y, Sui Y, Yu B. Investigation of a novel 24-slot/14-pole six-phase fault-tolerant modular permanent-magnet in-wheel motor for electric vehicles. *Energies* 2013;6:4980–5002.
- [56] Nounou K, Charpentier J, Marouani K, Benbouzid M, Kheloui A. Emulation of an electric naval propulsion system based on multiphase machine under healthy and faulty operating conditions. *IEEE Trans Veh Technol* 2018;67(8):6895–905.
- [57] Dos Santos D, Nguyen N, Semail E, Meinguet F, Guerin M. Dual-multiphase motor drives for fault-tolerant applications: Power electronic structures and control strategies. *IEEE Trans Power Electron* 2018;33(1):572–80.

- [58] Dai H, Jahns TM, Torres RA, Han D, Sarioglu B. Comparative evaluation of conducted common-mode EMI in voltage-source and current-source inverters using wide-bandgap switches. In *Proc. of the IEEE transportation electrification conference and expo (itec)*, 2018, p. 788–94.
- [59] Wei S, Zargari N, Wu B, Rizzo S. Comparison and mitigation of common mode voltage in power converter topologies. In *Proc. of the IEEE Industry Applications Conference, Vol. 3*, 2004, p. 1852–1857.
- [60] Fernandez M, Sierra-Gonzalez A, Robles E, Kortabarria I, Ibarra E, Martin J. New modulation technique to mitigate common mode voltage effects in star-connected five-phase AC drives. *Energies* 2020;13(3).
- [61] Han Y, Lu H, Li Y, Chai J. Analysis and suppression of shaft voltage in SiC-based inverter for electric vehicle applications. *IEEE Trans Power Electron* 2018;34(7):6276–85.
- [62] Park J, Wellawatta TR, Choi S, Hur J. Mitigation method of the shaft voltage according to parasitic capacitance of the PMSM. *IEEE Trans Ind Appl* 2017;53(5):4441–9.
- [63] Concari L, Barater D, Buticchi G, Concari C, Liserre M. H8 inverter for common-mode voltage reduction in electric drives. *IEEE Trans Ind Appl* 2016;52(5):4010–9.
- [64] Z. Shen TZ, Qu R. Dual-segment three-phase PMSM with dual inverters for leakage current and common-mode EMI reduction. *IEEE Trans Power Electron* 2019;34(6):5606–19.
- [65] Chen K, Hsieh M. Generalized minimum common-mode voltage PWM for two-level multiphase VSIs considering reference order. *IEEE Trans Power Electron* 2017;32(8):6493–509.
- [66] Chen J, Jiang D, Li Q. Attenuation of conducted EMI for three-level inverters through PWM. *CPSS Trans Power Electron Appl* 2018;3(2):134–45.
- [67] Yuen KK, Chung HS, Cheung VS. An active low-loss motor terminal filter for overvoltage suppression and common-mode current reduction. *IEEE Trans Power Electron* 2012;27(7):3158–72.
- [68] Acosta-Cambranis F, Zaragoza J, Romeral L, Berbel N. Comparative analysis of SVM techniques for a five-phase VSI based on SiC devices. *Energies* 2020;13(24):1–30.
- [69] Plazenet T, Boileau T, Caironi C, Nahid-Mobarakeh B. A comprehensive study on shaft voltages and bearing currents in rotating machines. *IEEE Trans Ind Appl* 2018;54(4):3749–59.
- [70] Willwerth A. To be considered “true inverter-duty”, motors need bearing protection. Technical report, Electro Static Technology; 2016, Motors need bearing protection.pdf.
- [71] Ahola J, Sarkimaki V, Muetze A, Tamminen J. Radio-frequency-based detection of electrical discharge machining bearing currents. *IET Electric Power Applications* 2011;5(4):386–92.
- [72] Euerle K, Iyer K, Severson E, Baranwal R, Tewari S, Mohan N. A compact active filter to eliminate common-mode voltage in a SiC-based motor drive. In *Proc. of the IEEE energy conversion congress and exposition (ecce)*, 2016, p. 1–8.
- [73] Matallana A, Ibarra E, Lopez I, Andreu J, Garate JI, Jorda X, Rebollo J. Power module electronics in HEV/EV applications: New trends in wide-bandgap semiconductor technologies and design aspects. *Renew Sustain Energy Rev* 2019;113:1–33.
- [74] Chen H, Zhao H. Review on pulse-width modulation strategies for common-mode voltage reduction in three-phase voltage-source inverters. *IET Power Electron* 2016;9(14):2611–20.
- [75] Mohammadpour A, Parsa L. A unified fault-tolerant current control approach for five-phase PM motors with trapezoidal back EMF under different stator winding connections. *IEEE Trans Power Electron* 2017;28(7):178–86.
- [76] Prieto B. Design and analysis of fractional-slot concentrated-winding multiphase fault-tolerant permanent magnet synchronous machines (Ph.D. thesis), Tecnum, Universidad de Navarra, Escuela de Ingenieros; 2015.
- [77] Karttunen J, Kallio S, Honkannen J, Peltoniemi P, Silventoinen P. Partial current harmonic compensation in dual three-phase PMSMs considering the limited available voltage. *IEEE Trans Ind Electron* 2017;64(2):1038–48.
- [78] Wang W, Zhang J, Cheng M, Li S. Fault-tolerant control of dual three-phase permanent-magnet synchronous machine drives under open-phase faults. *IEEE Trans Power Electron* 2017;32(3):2052–63.
- [79] Fabri G, Della Loggia E, Tursini M. Fault-tolerant design of motor-drives for high reliability applications. In *Proc. of the IEEE international forum on research and technologies for society and industry leveraging a better tomorrow (rtsi)*, 2015, p. 1–7.
- [80] Liu Z, Liu J, Li J. Modeling, analysis, and mitigation of load neutral point voltage for three-phase four-leg inverter. *IEEE Trans Ind Electron* 2013;60(5):2010–21.
- [81] da Silva IRFMP, ao Jacobina CB, Oliveira AC, de Almeida Carlos GA, ao de Rossiter Corrêa MB. Hybrid modular multilevel DSCC inverter for open-end winding induction motor drives. *IEEE Trans Ind Appl* 2017;53(2):1232–42.
- [82] Levi E, Jones M, Vukosavic SN, Toliyat HA. A novel concept of a multiphase, multimotor vector controlled drive system supplied from a single voltage source inverter. *IEEE Trans Power Electron* 2004;19(2):320–35.
- [83] Levi E. Multiphase electric machines for variable-speed applications. *IEEE Trans Ind Electron* 2008;55(5):1893–909.
- [84] Liu G, Lin Z, Zhao W, Chen Q, Xu G. Third harmonic current injection in fault-tolerant five-phase permanent-magnet motor drive. *IEEE Trans Power Electron* 2017;33(8):6970–9.
- [85] Xiong. A fault-tolerant FOC strategy for five-phase SPMSM with minimum torque ripples in the full torque operation range under double-phase open-circuit fault. *IEEE Trans Ind Electron* 2020;67(11):9059–72.
- [86] Durán MJ, Prieto J, Barrero F, Riveros JA, Guzman H. Space-vector PWM with reduced common-mode voltage for five-phase induction motor drives. *IEEE Trans Ind Electron* 2013;60(10):4159–68.
- [87] Liu Z, Zheng Z, Sudhoff SD, Gu C, Li Y. Reduction of common-mode voltage in multiphase two-level inverters using SPWM with phase-shifted carriers. *IEEE Trans Power Electron* 2016;31(9):6631–45.
- [88] Liu C, Chen Y, Yang Y, Liu Z. Principle and analysis of a five-phase six-leg switching power amplifier topology with fault-tolerant leg. In *Proc. of the IEEE international conference on cloud computing and intelligence systems (ccis)*, 2018, p. 532–6.
- [89] Liu C, Deng Z, Li K, Zhou J. One-cycle decoupling control method of multi-leg switching power amplifier for magnetic bearing system. *IET Electr Power Appl* 2019;13(8):1204–11.
- [90] Guo X, He R, Jian J, Lu Z, Sun X, Guerrero JM. Leakage current elimination of four-leg inverter for transformerless three-phase PV systems. *IEEE Trans Power Electron* 2016;31(3):1841–6.
- [91] Zhu R, Buticchi G, Liserre M. Investigation on common-mode voltage suppression in smart transformer-fed distributed hybrid grids. *IEEE Trans Power Electron* 2018;33(10):8438–48.
- [92] Li A, Jiang D, Gao Z, Kong W, Jia S, Qu R. Three-phase four-leg drive for DC-biased sinusoidal current Vernier reluctance machine. *IEEE Trans Ind Appl* 2019;55(3):2758–69.
- [93] Wang W, Zhang J, Cheng M. Common model predictive control for permanent-magnet synchronous machine drives considering single-phase open-circuit fault. *IEEE Trans Power Electron* 2017;32(7):5862–72.
- [94] Zhou X, Li H, Lu M, Zeng F. PMSM open-phase fault-tolerant control strategy based on four-leg inverter. *IEEE Trans Power Electron* 2020;35(3):2799–808.
- [95] Djeriou A, Houari A, Saim A, Ait-Ahmed M, Pierfederici S, Benkhoris MF, Machmoum M, Ghanes M. Flatness-based grey wolf control for load voltage unbalance mitigation in three-phase four-leg voltage source inverters. *IEEE Trans Ind Appl* 2020;56(2):1869–81.
- [96] Tran T, Raisz D, Monti A. Harmonic and unbalanced voltage compensation with VOC-based three-phase four-leg inverters in islanded microgrids. *IET Power Electron* 2020;13(11):2281–92.
- [97] R. Zhang DB, Lee FC. Three-dimensional space vector modulation for four-leg voltage-source converters. *IEEE Trans Power Electron* 2002;17(3):314–26.
- [98] Llonch-Masachs M, Heredero-Peris D, Montesinos-Miracle D, Rull-Duran J. Understanding the three and four-leg inverter space vector. In *Proc. of the European conference on power electronics and applications (EPE ECCE Europe)*, 2016, p. 1–10.
- [99] Zhang F, Yan Y. Selective harmonic elimination PWM control scheme on a three-phase four-leg voltage source inverter. *IEEE Trans Power Electron* 2009;24(7):1682–9.
- [100] Zhang M, Atkinson DJ, Ji B, Armstrong M, Ma M. A near-state three-dimensional space vector modulation for a three-phase four-leg voltage source inverter. *IEEE Trans Power Electron* 2014;29(11):5715–26.
- [101] Hou C, Wang P, Chen C, Chang C. Common mode voltage reduction in four-leg inverter with multicarrier PWM scheme. In *Proc. of the international conference on power electronics and ecce asia (icpe - ecce)*, 2019, p. 3223–8.
- [102] Eldeeb H, Abdel-Khalik A, Kullick J, Hackl C. Pre- and postload current control of dual three-phase reluctance synchronous drives. *IEEE Trans Ind Electron* 2020;67(5):3361–73.
- [103] Xiao L, Zhang L, Gao F, Quian J. Robust fault-tolerant synergetic control for dual three-phase PMSM drives considering speed sensor fault. *IEEE Access* 2020;8:78912–22.
- [104] Sala G, Gerada D, Gerada C, Tani A. Radial force control for triple three-phase sectored SPM machines. Part II: Open winding fault tolerant control. In *Proc. of the IEEE workshop on electrical machines design, control and diagnosis (wemdc)*, 2017, p. 275–80.
- [105] Miyama Y, Ishizuka M, Kometani H, Akatsu K. Vibration reduction by applying carrier phase-shift PWM on dual three-phase winding permanent magnet synchronous motor. *IEEE Trans Ind Appl* 2018;54(6):5998–6004.
- [106] Hu Y, Huang S, Wu X, Li X. Control of dual three-phase permanent magnet synchronous machine based on five-leg inverter. *IEEE Trans Power Electron* 2019;34(11):11071–9.
- [107] Karttunen J, Kallio S, Peltoniemi P, Silventoinen P, Pyrhonen O. Dual three-phase permanent magnet synchronous machine supplied by two independent voltage source inverters. In *Proc. of the international symposium on power electronics, electrical drives, automation and motion (speedam)*, 2012, p. 741–746.
- [108] Shen Z, Jiang D, Liu Z, Ye D, Li J. Common-mode voltage elimination for dual two-level inverter-fed asymmetrical six-phase PMSM. *IEEE Trans Power Electron* 2020;35(4):3828–40.
- [109] Han D, Morris CT, Sarioglu B. Common-mode voltage cancellation in PWM motor drives with balanced inverter topology. *IEEE Trans Ind Electron* 2017;64(4):2683–8.

- [110] Han D, Lee W, Li S, Sarlioglu B. New method for common mode voltage cancellation in motor drives: Concept, realization, and asymmetry influence. *IEEE Trans Power Electron* 2018;33(2):1188–201.
- [111] Hu W, Ruan C, Nian H, Sun D. Simplified modulation scheme for open-end winding PMSM system with common DC bus under open-phase fault based on circulating current suppression. *IEEE Trans Power Electron* 2020;35(1):10–4.
- [112] Lin X, Huang W, Wang L. SVPWM Strategy based on the hysteresis controller of zero-sequence current for three-phase open-end winding PMSM. *IEEE Trans Power Electron* 2019;34(4):3474–86.
- [113] Saghafinia A. Recent developments on power inverters. *IntechOpen*; 2017.
- [114] Oleschuk V, Ermuratshii V. Open-end winding multiphase installation regulated by modified techniques of space-vector PWM. In *Proc. of the IEEE Ukraine conference on electrical and computer engineering (ukrcon)*, 2019, p. 299–304.
- [115] Karampuri R, Jain S, Somasekhar VT. Common-mode current elimination PWM strategy along with current ripple reduction for open-winding five-phase induction motor drive. *IEEE Trans Power Electron* 2019;34(7):6659–68.
- [116] Baoji Wang CS, Cao R. Research on the filters for dual-inverter fed open-end winding transformer topology in photovoltaic grid-tied applications. *Energies* 2019;12(2338):1–22.
- [117] Pramanick S, Azeez NA, Sudharshan Kaarthik R, Gopakumar K, Cecati C. Low-order harmonic suppression for open-end winding IM with dodecagonal space vector using a single DC-link supply. *IEEE Trans Ind Electron* 2015;62(9):5340–7.
- [118] Baranwal R, Basu K, Mohan N. Carrier-based implementation of SVPWM for dual two-level VSI and dual matrix converter with zero common-mode voltage. *IEEE Trans Power Electron* 2015;30(3):1471–87.
- [119] Mekasser M, Gao Q, Xu C. Common mode voltage elimination in dual-inverter-fed six-phase open-end winding PMSM drives with a single DC supply. *J Eng* 2019;2019(17):3598–602.
- [120] Zhang F, Zhu L, Jin S, Su X, Ademi S, Cao W. Controller strategy for open-winding brushless doubly fed wind power generator with common mode voltage elimination. *IEEE Trans Ind Electron* 2019;66(2):1098–107.
- [121] Rahman K, Iqbal A, Al-Emadi N, Ben-Brahim L, Al-ammari R, Dehghani Tafti H. Common mode voltage reduction in open-end multi-phase load system fed through matrix converter. In *Proc. of the IEEE energy conversion congress and exposition (ecce)*, 2016, p. 1–6.
- [122] A. Iqbal MM, Abu-Rub H. Finite set model predictive current control with reduced and constant common mode voltage for a five-phase voltage source inverter. In *Proc. of the international symposium on industrial electronics (isie)*, 2014, p. 479–84.
- [123] Dabour SM, Abdel-Khalik AS, Massoud AM, Ahmed S. Analysis of scalar PWM approach with optimal common-mode voltage reduction technique for five-phase inverters. *IEEE J Emerg Sel Top Power Electron* 2019;7(3):1854–71.
- [124] Levi E, Barrero F, Duran MJ. Multiphase machines and drives - revisited. *IEEE Trans Ind Electron* 2016;63(1):429–32.
- [125] Samanes J, Gubia E, Juanakorena X, Girones C. Common-mode and phase-to-ground voltage reduction in back-to-back power converters with discontinuous PWM. *IEEE Trans Ind Electron* 2020;67(9):7499–508.
- [126] Prieto J, Jones M, Barrero F, Levi E, Toral S. Comparative analysis of discontinuous and continuous PWM techniques in VSI-fed five-phase induction motor. *IEEE Trans Ind Electron* 2011;58(12):5324–35.
- [127] Yun S-W, Baik J-H, Kim D-S, Yoo J-Y. A new active zero state PWM algorithm for reducing the number of switchings. *J Power Electron* 2017;17:88–95.
- [128] Cacciato M, Consoli A, Scarcella G, Testa A. Reduction of common-mode currents in PWM inverter motor drives. *IEEE Trans Ind Appl* 1999;35(2):469–76.
- [129] Baik J, Yun S, Kim D, Kwon C, Yoo J. Remote-state PWM with minimum RMS torque ripple and reduced common-mode voltage for three-phase VSI-fed BLAC motor drives. *Electronics* 2020;9(586):1–17.
- [130] y A. M. Hava EU. A near-state PWM method with reduced switching losses and reduced common-mode voltage for three-phase voltage source inverters. *IEEE Trans Ind Appl* 2009;45(2):782–93.
- [131] Hava AM, Ün E. A high performance PWM algorithm for common mode voltage reduction in three-phase voltage source inverters. *IEEE Trans Power Electron* 2011;26(7):1998–2008.
- [132] Duran MJ, Barrero F, Prieto J. Dc-bus utilization and overmodulation performance of five-phase voltage source inverters using model predictive control. In: *Proc. of the IEEE international conference on industrial technology*. 2010, p. 1501–6. <http://dx.doi.org/10.1109/ICIT.2010.5472477>.
- [133] Salem A, Narimani M. A review on multiphase drives for automotive traction applications. *IEEE Trans Transp Electr* 2019;5(4):1329–48.
- [134] Iqbal A, Levi E. Space vector modulation schemes for a five-phase voltage source inverter. In *Proc. of the European conference on power electronics and applications (EPE ECCE Europe)*, 2005, p. 1–12.
- [135] Dujic D, Jones M, Levi E. Continuous carrier-based vs. Space vector PWM for five-phase VSI. In *Proc. of the international conference on "computer as a tool" (eurocon)*, 2007, p. 1772–1779.
- [136] Dujic D, Jones M, Levi E, Prieto Corvalán J, Barrero F. Switching ripple characteristics of space vector PWM schemes for five-phase two-level voltage source inverters - Part 1: Flux harmonic distortion factors. *IEEE Trans Ind Electron* 2011;58(7):2789–98.
- [137] Prieto J, Barrero F, Toral S, Jones M, Levi E. Analytical evaluation of switching characteristics in five-phase drives with discontinuous space vector pulse width modulation techniques. In *Proc. of the European conference on power electronics and applications (EPE ECCE Europe)*, 2011, p. 1–10.
- [138] Wang F. Sine-triangle versus space-vector modulation for three-level pwm voltage-source inverters. *IEEE Trans Ind Appl* 2002;38(2):500–6.
- [139] Liu Z, Wang P, Sun W, Shen Z, Jiang D. Sawtooth carrier-based PWM methods with common-mode voltage reduction for symmetrical multiphase two-level inverters with odd phase number. *IEEE Trans Power Electron* 2021;36(1):1171–83.
- [140] Fernandez M, Robles E, Kortabarria I, Andreu J, Ibarra E. Novel modulation techniques to reduce the common mode voltage in multiphase inverters. In *Proc. of the annual conference of the IEEE industrial electronics society (IECON)*, 2019, p. 1898–903.
- [141] Wang W, Fan Y, Chen S, Zhang Q. Finite control set model predictive current control of a five-phase PMSM with virtual voltage vectors and adaptive control set. *CES Trans Electr Mach Syst* 2018;2(1):136–41.
- [142] Luo Y, Liu C. Elimination of harmonic currents using a reference voltage vector based-model predictive control for a six-phase PMSM motor. *IEEE Trans Power Electron* 2019;34(7):6960–72.
- [143] Liu G, Song C, Chen Q. FCS-Mpc-based fault-tolerant control of five-phase IPMSM for MTPA operation. *IEEE Trans Power Electron* 2020;35(3):2882–94.
- [144] Zhao W, Tao T, Zhu J, Tan H, Du Y. A novel finite-control-set model predictive current control for five-phase PM motor with continued modulation. *IEEE Trans Power Electron* 2020;35(7):7261–70.
- [145] Guo L, Jin N, Gan C, Xu L, Wang Q. An improved model predictive control strategy to reduce common-mode voltage for two-level voltage source inverters considering dead-time effects. *IEEE Trans Ind Electron* 2019;66(5):3561–72.
- [146] Kouro S, Cortes P, Vargas R, Ammann U, Rodriguez J. Model predictive control - a simple and powerful method to control power converters. *IEEE Trans Ind Electron* 2009;56(6):1826–38.
- [147] Duran MJ, Riveros JA, Barrero F, Guzman H, Prieto J. Reduction of common-mode voltage in five-phase induction motor drives using predictive control techniques. *IEEE Trans Ind Appl* 2012;48(6):2059–67.
- [148] Xu W, Zou J, Liu Y, Zhu J. Weighting factorless model predictive thrust control for linear induction machine. *IEEE Trans Power Electron* 2019;34(10):9916–28.
- [149] Yu B, Song W, Li J, Li B, Saeed M. Improved finite control set model predictive current control for five-phase VSIs. *Trans Power Electron* 2021;36(6):7038–48.
- [150] Yu B, Song W, Guo Y, Li J, Saeed MSR. Virtual voltage vector-based model predictive current control for five-phase VSIs with common-mode voltage reduction. *IEEE Trans Transp Electr* 2021;7(2):706–17.
- [151] López O, Álvarez J, Malvar J, Yepes AG, Vidal A, Baneira F, Pérez-Estévez D, Freijedo FD, Doval-Gandoy J. Space-vector PWM with common-mode voltage elimination for multiphase drives. *IEEE Trans Power Electron* 2016;31(12):8151–61.
- [152] Dordevic O, Jones M, Levi E. A comparison of carrier-based and space vector PWM techniques for three-level five-phase voltage source inverters. *IEEE Trans Ind Inform* 2013;9(2):609–19.